ISSN 1814-4225 (print)
ISSN 2663-2012 (online)

UDC 621.396

doi: 10.32620/reks.2024.3.08

Eduard TSERNE, Semen ZHYLA, Anatoliy POPOV, Dmytro VLASENKO, Denys KOLESNIKOV, Olha INKARBAIEVA, Volodymyr KOSHARSKYI, Hlib CHEREPNIN

National Aerospace University "Kharkiv Aviation Institute", Kharkiv, Ukraine

ON-BOARD RADAR COMPLEX FOR HIGH-PRECISION DIRECTION FINDING OF RADIO SOURCES FOR AUTONOMOUS GUIDANCE OF WINGED UAVS

The subject *of this article is the design of a cheap, simple, and highly accurate on-board radar system for determining the angular position of radio-signal emission stations, which can be used to guide UAVs to a specified area of space.* ***The aim*** *of this study is to develop high-precision functioning algorithms, practical recommendations for implementation, and experimental measurements of the main parameters of the onboard radio direction finders of radio radiation sources placed on winged UAVs.* ***Objectives*** *of the research: 1) analysis of the statistical theory of optimization of signal processing algorithms in radar systems; 2) synthesis of direction-finding algorithms for radio measurement sources capable of performing measurements with high accuracy and in a wide range of unambiguous measurement angles; 3) synthesis of the radio direction finder structural scheme and its simulation modelling; 4) design of radio direction finder receiving antennas capable of operating separately and in a complex; 5) justification of the choice of components for the input paths of receivers, parameters of ADC and microcomputers that make up the main components of the radar complex; 6) manufacturing of a working model of the radar complex; 7) experimental measurements in the laboratory.* ***The methods*** *for solving the tasks are based on the statistical theory of optimization of radio engineering systems for remote sensing and radar, existing software tools for simulation modelling, and the theory of radio measurements. The main idea behind creating a cheap, simple, and highly accurate on-board radar system for radio emitter direction finding is to combine the results of angular position measurements from several amplitude and phase meters. This* ***approach*** *allows us to create an easy-to-implement radio system with the advantages of different measuring instruments.* ***The following results were obtained:*** *1) theoretical studies and simulation modelling confirmed that by combining measurements from a two-antenna amplitude direction finder with narrow diagrams, a two-antenna direction finder with wide diagrams, and a two-antenna phase finder, it is possible to achieve both high accuracy and a wide range of unambiguous measurements; 2) a radar system based on a cheap and commonly available element base was developed; 3) antennas were developed that can be easily installed under the wings of UAVs; 4) experimental studies confirmed the performance of complex signal processing in an on-board six-antenna radio direction finder. The material of this work forms the basis for further experimental development of radio-direction finders for various purposes, opens up opportunities for overcoming the contradiction between accuracy and range of unambiguous measurements, and highlights an additional direction for increasing the autonomy of winged UAVs.*

Keywords: *multi-antenna radio direction finders, statistical optimisation of algorithms, experimental development of radiometers, installation of antennas on UAVs.*

1. Introduction

Motivation. One of the essential parts of radio equipment that every modern aerodrome should be equipped with is an aerodrome non-directional radio beacon [1]. The task of the beacon is to guide aircraft and helicopters to the aerodrome area, perform pre-landing manoeuvres, and maintain direction along the runway axis. Today, aviation uses non-directional radio beacons of various modifications and companies, and the problem of guiding an aircraft to a given point has been studied for many years [2, 3]. With the development of unmanned aerial vehicles, their introduction into cargo delivery systems, long-distance data transmission, and surveillance of large areas of space, the issue of guiding UAVs to their area of operation or their autonomous return to the launch site has also become relevant [4, 5]. At the same time, the creation of a beacon direction-finding system from UAV and UAV flight control systems has its own peculiarities.

Compared to aircraft or helicopters, UAVs have limited overall dimensions for equipment placement and complex structural design features. The frequencies for control and data exchange with unmanned aerial vehicles are highly variable and are not coordinated with airfields [6, 7]. The UAV take-off and landing point is

not equipped with special facilities or technical equipment. The price of on-board electronic equipment is rapidly increasing and often exceeds the price of the carrier.

Given these features, the task of creating an on-board radio direction finder that ergonomically fits into the UAV design, has high accuracy and a wide range of angles for unambiguous measurement of directions to beacons, and is characterized by small weight, dimensions, and ease of implementation becomes relevant.

State of the Art. To bring the aircraft to the point of beacon emission, the angular position of the radio source is first measured. To estimate the direction, radio direction finders are usually used based on the amplitude comparison, delay time measurement, propagation spectrum estimation, interferometric signal processing, and Doppler frequency shift. Let us consider them in more detail.

The principle of operation of amplitude radio direction finders is to compare the amplitudes of the received signals, which are proportional to the spatial characteristics of the receiving antennas in the direction in which the radio source is located [8, 9]. The main stages of signal processing for direction finding are clear, and radio direction finders are relatively easy to implement, small, light in weight, and inexpensive. The disadvantages include the low accuracy of the angular position measurement, dependence of measurements on polarization, and distortion of the radio wave front.

Interferometric direction finders are based on measurements of the phase difference between two spatially separated antennas that receive signals from a point source of radio radiation [10, 11]. Such direction finders are widely used in practice and are manufactured by foreign companies. The advantages of phase direction finders are the simplicity of implementing the antenna system and the bearing reference algorithm, and the resistance to parasitic amplitude modulation. The disadvantages include the complexity of implementing a receiver with completely identical phase characteristics and a narrow range of unambiguous measurement angles.

A type of interferometric direction finder is a correlation-interferometric direction finder that uses an annular antenna array with sequential switching of antenna elements and algorithms for correlation processing of measured complex amplitudes on antenna pairs to measure the angle [12, 13]. The advantages of this method include high sensitivity and accuracy of direction finding; however, the cost of implementing multi-channel receivers and the complexity of signal processing in digital processors make it impractical to widely use correlation-interferometric direction finders [14].

Doppler direction finders measure the shift in the Doppler frequency caused by the movement or rotation of the receiving antenna [15]. The greatest effect of this method is achieved when the antenna is fully moved toward the incoming wave. Doppler direction finding usually does not involve direct rotation of the direction-finding antenna, which is technically difficult to achieve [16]. The method consists of installing several antennas in a series of concentric circles, and an electronic switch quickly connects each antenna in a sequence that is equivalent to rotating the direction finder to the antenna [17]. Doppler direction finders have high sensitivity, high accuracy, weak dependence on wave polarisation, and are not sensitive to wave front distortion [18, 19]. The disadvantage of the Doppler direction finding system is its low efficiency in dealing with interference. The system is still under development, and its improvement will lead to a more complex system, and the cost will increase accordingly.

The accuracy of phase direction finding is inversely proportional to the distance between the direction finder antennas, but the maximum antenna size is limited by the wavelength of the measured electromagnetic waves. To overcome this contradiction, long-base direction finders are used, but the measurement parameter is the delay time rather than the phase shift [20, 21]. The advantages of such systems include high accuracy, insensitivity to polarization, and no measurement ambiguity. The disadvantages include large separation distances of the meters and the need to use signals with a certain type of modulation [22].

Radio direction finders, which estimate the spatial position based on the measurement results of the spatial spectrum of the received signals, consist of a set of antennas and multi-channel coherent receivers that record the amplitudes and phases of the received signals [23]. Further processing of the measurement vector was performed in a digital processor using correlation analysis. The technology of spatial spectrum estimation and direction finding can implement the simultaneous direction finding of several radiation sources whose signals exist in the same channel at the same time, and it is also possible to implement direction finding with super-resolution [24]. Only some signal samples are required to accurately determine the direction; thus, this method is suitable for finding direction signals with frequency jumps. In general, it can be stated that there is high sensitivity and high accuracy; the antenna array can be implemented using elements of any orientation, and the requirements for the accuracy of the position of these elements are not high [25]. The above advantages of direction finders with spatial spectrum estimation solve problems that have long existed in previously discussed methods. This direction finder requires broadband input paths, and consistent electrical characteristics for each

ISSN 1814-4225 (print)
ISSN 2663-2012 (online)

antenna array element and multichannel receiver. In addition, high-performance computing processors are required to solve practical problems.

Problem statement. Based on the analysis of current scientific research and the above contradictions, the actual scientific problem is designing a radio direction finder that has small weight and size characteristics, is ergonomically placed on a UAV, measures the angular positions of a radio source with high accuracy and in a wide range of angles, and is simple and cheap to implement.

To achieve the stated goals of the work, it was necessary to solve and complete the following tasks:

1) to analyse theoretical approaches to the statistical synthesis of optimal direction finding algorithms (Section 2);

2) to develop an easy-to-implement and accurate method for the direction finding of radio sources at various unambiguous measurement angles (Section 3);

3) to develop of a structural diagram of an optimal on-board directional beacon meter and its simulation modelling in DataFlow mode (Section 4);

4) to design of radio direction finder antennas (Section 5); and

5) to justify the selection of components for the input paths of the receivers (Section 6); and

6) to implement the experimental model of the direction finding complex and confirming the main results obtained from experimental measurements (Section 7).

2. Theoretical basis of structural synthesis of radio-measuring systems

To solve the optimisation problems of synthesising signal processing algorithms in multichannel radio-direction finders, we use the statistical theory of optimisation for radio-engineering systems for remote sensing and radar. According to this theory, it is advisable to use the maximum-likelihood function method to solve this problem. The essence of this method is to find the parameter λ that maximises the likelihood function $P[\vec{u}(t)|\lambda]$ [26], which is the conditional probability density function of a random process $\vec{u}(t)$ at a fixed value of parameter λ. Instead of function $P[\vec{u}(t)|\lambda]$, its logarithm is often maximised, since the logarithm function is monotonic and does not change the maximum point $P[\vec{u}(t)|\lambda]$ [27, 28]. To determine the optimal estimates of parameter λ, it is necessary to solve the following system of equations

$$\left.\frac{d\ln P[\vec{u}(t)|\lambda]}{d\lambda}\right|_{\lambda=\lambda_{true}} = 0, \qquad (1)$$

where $\frac{d}{d\lambda}$ is the operator of the derivative, which is taken at the point of the true value λ_{true} of parameter λ; $\vec{u}(t)$ is the observation equation, including the received useful signals distorted by the receiver noise.

The general form of the observation equations in multi-antenna radio direction finders when estimating the direction to the radio source θ_s is as follows

$$\vec{u}(t) = \mathrm{Re}\{\dot{\vec{s}}(t,\theta_s)\} + \vec{n}(t), \qquad (2)$$

where

$$\vec{u}(t) = \|u_1(t),\, u_2(t),\, ...,\, u_N(t)\|, \qquad (3)$$

$\mathrm{Re}\{\cdot\}$ is the operator of the real part of the vector of the received useful complex signals $\dot{\vec{s}}(t,\theta_s)$,

$$\dot{\vec{s}}(t,\theta_s) = \|\dot{s}_1(t,\theta_s),\, \dot{s}_2(t,\theta_s),\, ...,\, \dot{s}_N(t,\theta_s)\|, \qquad (4)$$

$$\dot{s}_i(t,\theta_s) = \\ = K_{0i}\int_{\Theta}\dot{G}_i(\theta-\theta_{0i})\delta(\theta-\theta_s)\dot{A}(t)e^{-j2\pi f_0 t}e^{j\psi_i(\theta_s)}d\theta, \qquad (5)$$

$\psi_i(\theta_s) = 2\pi f_0 \Delta r_i(\theta_s) c^{-1}$ is the phase shift of the signal in each receiving channel relative to the phase centre of the antenna field; $\Delta r_i(\theta_s)$ is the difference in distances passed by electromagnetic waves from the source to each antenna; $\delta(\theta-\theta_s)$ is the delta function that determines the spatial position of the point source of radio emission in the direction θ_s; K_{0i} is the gain of the i-th receiving channel; $\dot{G}_i(\theta-\theta_{0i})$ is the radiation pattern of the i-th antenna, which is oriented with its maximum in the direction of θ_{0i}; $\dot{A}(t)$ is the complex envelope of the signal emitted by the source; $e^{-j2\pi f_0 t}$ is a harmonic oscillation in complex form with a carrier frequency f_0; t is time; θ is the angular coordinates; c is the propagation speed of electromagnetic waves; $i = \overline{1,N}$;

$$\vec{n}(t) = \|n_1(t),\, n_2(t),\, ...,\, n_N(t)\| \qquad (6)$$

is internal noise.

The geometrical underlying model (5) is shown in Fig. 1. From this model, it follows that the input paths differ only in the gains K_{0i}.

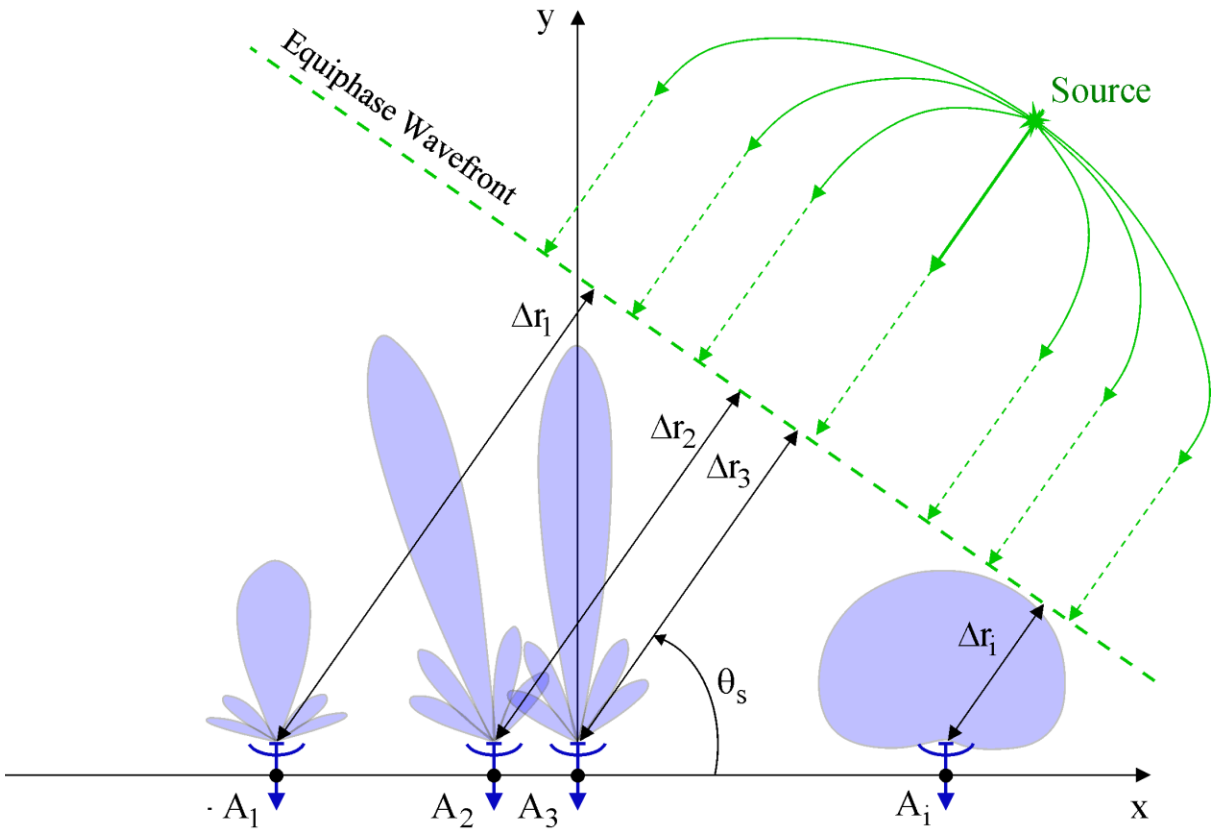

Fig. 1. General geometry of measurements in radio direction finders

The internal noises in the receiving paths $n_i(t)$ are assumed to be white Gaussian noise, which are uncorrelated but have the same spectral power density $0.5N_0$. The correlation function of the internal noise has the following form

$$R_{n_i}(t_1 - t_2) = 0.5N_0\delta(t_1 - t_2), \qquad (7)$$

where $\delta(t_1 - t_2)$ is the delta function.

One of the most important steps in solving an optimization problem is to determine $P[\vec{u}(t)\,|\,\lambda]$. A previous study [26] presented a methodology for constructing likelihood functions for a wide range of radio location and remote sensing problems. In this study, we use the following likelihood function:

$$P[\vec{u}(t)\,|\,\lambda = \theta_s] = \kappa \exp\left\{-\frac{1}{N_0}\sum_{i=1}^{N}\int_T \left[u_i(t) - \mathrm{Re}\{\dot{s}_i(t,\theta_s)\}\right]^2 dt\right\}, \qquad (8)$$

where κ is a coefficient that does not depend on the parameters to be estimated; T is the observation time. Parameter $\lambda = \theta_s$ is a constant value.

By substituting (8) into (7), we obtain a system of likelihood equations

$$\frac{2}{N_0}\sum_{i=1}^{N}\int_T \left[u_i(t) - \mathrm{Re}\{\dot{s}_i(t,\theta_s)\}\right]\mathrm{Re}\left\{\frac{d\dot{s}_i(t,\theta_s)}{d\theta_s}\right\}dt = 0,$$

or

$$\sum_{i=1}^{N}\int_T u_i(t)\,\mathrm{Re}\left\{\frac{d\dot{s}_i(t,\theta_s)}{d\theta_s}\right\}dt = \sum_{i=1}^{N}\int_T \mathrm{Re}\{\dot{s}_i(t,\theta_s)\}\,\mathrm{Re}\left\{\frac{d\dot{s}_i(t,\theta_s)}{d\theta_s}\right\}dt. \qquad (9)$$

The left part of (9) defines the basic optimal operations to be performed on the received oscillations $u_i(t)$ in each channel. The left part must be compared with the right part. The right panel shows the observational characteristics of the multichannel radio direction finder, which shows the response of the meter to changes in the angular position θ_s of the radiation source.

After determining the measurement conditions and type of radio direction finder, or a combination of several, it is possible to synthesize an optimal algorithm for the direction finding of radio sources. We will perform such an optimization of the radio-direction finder structure by considering the defined scientific problem.

ISSN 1814-4225 (print)
ISSN 2663-2012 (online)

3. Optimal Method for High-Precision Direction Finding of Radio Sources in a Wide Range of Unambiguous Measurement Angles

We perform statistical synthesis of the signal processing method in a radio-direction finder that meets contradictory requirements. It should have a small weight and dimensions, ergonomic placement on board, high accuracy, a wide range of unambiguous measurement angles, simple implementation, and low cost. To meet these requirements, we used a combination of the following three radio direction finders: an amplitude radio direction finder with wide-directional antennas, an amplitude radio direction finder with narrow-directional antennas, and a phase radio direction finder with omni-directional antennas. The measurement geometry is shown in Fig. 2.

Useful signals have the following models:

$$\dot{s}_1(t,\theta_s) = K_{01} \times$$
$$\times \int_{\Theta} G_1(\theta-\theta_b-0.5\theta_{\delta 1})\delta(\theta-\theta_s)\dot{A}(t)e^{-j2\pi f_0 t}d\theta, \quad (10)$$

$$\dot{s}_2(t,\theta_s) = K_{02} \times$$
$$\times \int_{\Theta} G_1(\theta-\theta_b+0.5\theta_{\delta 1})\delta(\theta-\theta_s)\dot{A}(t)e^{-j2\pi f_0 t}d\theta, \quad (11)$$

$$\dot{s}_3(t,\theta_s) = K_{03} \times$$
$$\times \int_{\Theta} G_2(\theta-\theta_b-0.5\theta_{\delta 2})\delta(\theta-\theta_s)\dot{A}(t)e^{-j2\pi f_0 t}d\theta, \quad (12)$$

$$\dot{s}_4(t,\theta_s) = K_{04} \times$$
$$\times \int_{\Theta} G_2(\theta-\theta_b+0.5\theta_{\delta 2})\delta(\theta-\theta_s)\dot{A}(t)e^{-j2\pi f_0 t}d\theta, \quad (13)$$

$$\dot{s}_5(t,\theta_s) =$$
$$= K_{05}G_3(\theta_b)\dot{A}(t)e^{-j2\pi f_0\left(t-\frac{1}{2}\frac{d\cos(\theta_s-\theta_b)}{c}\right)}, \quad (14)$$

$$\dot{s}_6(t,\theta_s) =$$
$$= K_{06}G_3(\theta_b)\dot{A}(t)e^{-j2\pi f_0\left(t+\frac{1}{2}\frac{d\cos(\theta_s-\theta_b)}{c}\right)}, \quad (15)$$

where $G_1(\theta-\theta_b-0.5\theta_{\delta 1})$ and $G_1(\theta-\theta_b+0.5\theta_{\delta 1})$ are identical in shape to the radiation patterns of wide-directional antennas that are spaced apart in space by an angle $\theta_{\delta 1}$ from the equal-signal direction θ_b; $G_2(\theta-\theta_b-0.5\theta_{\delta 2})$ and $G_2(\theta-\theta_b+0.5\theta_{\delta 2})$ are identical in shape, but spaced apart in space by an angle $\theta_{\delta 2}$ from the equal-signal direction θ_b of the narrowly focused antenna pattern; $G_3(\theta_b)$ is the gain of the phase-direction finder antenna in the direction θ_b, d is the distance between the phase-direction finder antennas placed in the same line along the axis x.

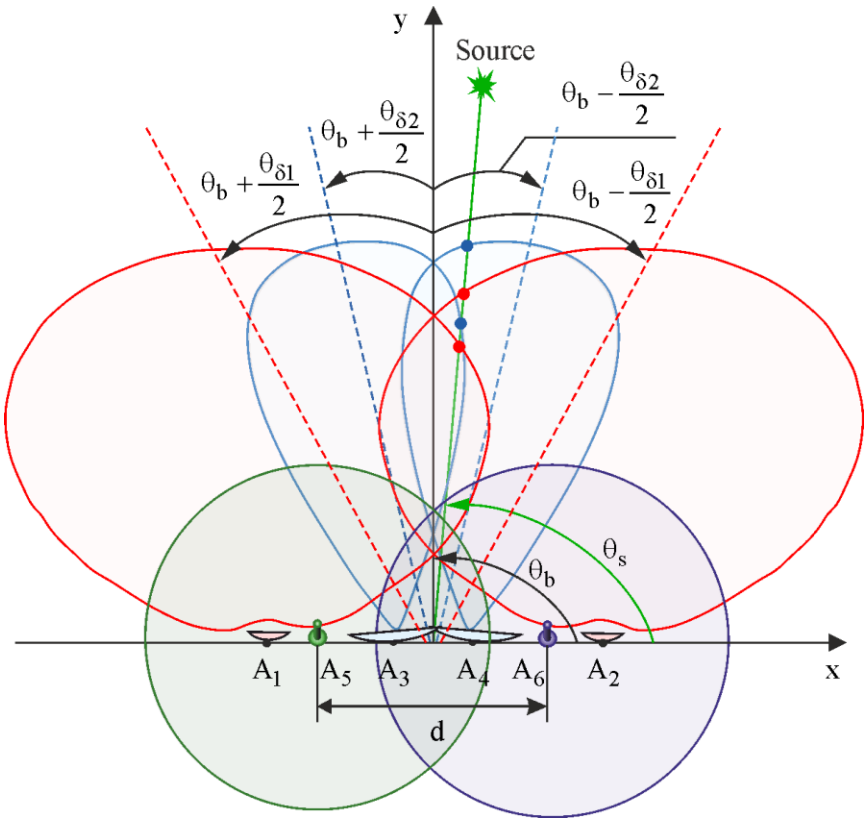

Fig. 2. Measurement geometry in a six-antenna direction finder

In the signal models (10-15) observed in amplitude direction finders, there is no information about the phase shift between antennas, whereas in phase direction finders, all information about the angular position of the source is contained in the phase and cannot be observed in amplitude multipliers.

Substituting the observation equations, consisting of an additive mixture of useful signals (10) and delta-correlated noises (6), into inequality (9), we obtain

$$\left.\frac{dG_1(\theta-\theta_b-0.5\theta_{\delta1})}{d\theta}\right|_{\theta=\theta_s} K_{01}\int_T u_1(t)\dot{h}(t)dt +$$
$$+\left.\frac{dG_1(\theta-\theta_b+0.5\theta_{\delta1})}{d\theta}\right|_{\theta=\theta_s} K_{02}\int_T u_2(t)\dot{h}(t)dt \mp$$
$$+\left.\frac{dG_2(\theta-\theta_b-0.5\theta_{\delta2})}{d\theta}\right|_{\theta=\theta_s} K_{03}\int_T u_3(t)\dot{h}(t)\,dt +$$
$$+\left.\frac{dG_2(\theta-\theta_b+0.5\theta_{\delta2})}{d\theta}\right|_{\theta=\theta_s} K_{04}\int_T u_4(t)\dot{h}(t)dt -$$
$$-G_3(\theta_b)\sin(\theta_s-\theta_b)\times$$
$$\times\left(\cos\left(\pi f_0\frac{d\cos(\theta_s-\theta_b)}{c}\right)+j\sin\left(\pi f_0\frac{d\cos(\theta_s-\theta_b)}{c}\right)\right)\times$$
$$\times\left(j\pi f_0 dc^{-1}\right)K_{05}\int_T u_5(t)\dot{h}(t)dt +$$
$$+G_3(\theta_b)\sin(\theta_s-\theta_b)\times$$
$$\times\left(\cos\left(\pi f_0\frac{d\cos(\theta_s-\theta_b)}{c}\right)-j\sin\left(\pi f_0\frac{d\cos(\theta_s-\theta_b)}{c}\right)\right)\times$$
$$\times\left(j\pi f_0 dc^{-1}\right)K_{06}\int_T u_6(t)\dot{h}(t)dt =$$
$$=K_{01}\left.\frac{dG_1(\theta-\theta_b-0.5\theta_{\delta1})}{d\theta}\right|_{\theta=\theta_s} G_1(\theta_s-\theta_b+0.5\theta_{\delta1})\frac{1}{2}E_s +$$
$$+K_{02}\left.\frac{dG_1(\theta-\theta_b+0.5\theta_{\delta1})}{d\theta}\right|_{\theta=\theta_s} G_1(\theta_s-\theta_b-0.5\theta_{\delta1})\frac{1}{2}E_s +$$
$$+K_{03}\left.\frac{dG_2(\theta-\theta_b-0.5\theta_{\delta2})}{d\theta}\right|_{\theta=\theta_s} G_2(\theta_s-\theta_b+0.5\theta_{\delta2})\frac{1}{2}E_s +$$
$$+K_{04}\left.\frac{dG_2(\theta-\theta_b+0.5\theta_{\delta2})}{d\theta}\right|_{\theta=\theta_s} G_2(\theta_s-\theta_b-0.5\theta_{\delta2})\frac{1}{2}E_s +$$
$$+(K_{06}-K_{05})G_3^2(\theta_b)\sin(\theta_s-\theta_b)\left(\pi f_0\frac{d}{c}\right)\frac{1}{2}E_s\ , \quad (16)$$

where $\dot{h}(t)=\dot{A}(t)e^{-j2\pi f_0 t}$ is a transmission coefficient of the optimal filter; $E_s=\int_T|\dot{A}(t)|^2dt$ is the energy of the signal emitted by the source.

The left-hand side of (16) shows the optimal operations to be performed on the received signals $\ddot{u}(t)$ in each receiving channel of the direction finder. The first four equations describe the processing in the amplitude direction finders. In each channel, it is necessary to perform matched filtering of the received observations using a filter with a pulse response $\dot{h}(t)$. The filtering results are then multiplied by the weighting coefficients K_{0i} and the slope of the radiation patterns, which are determined by the following equation

$$\left.\frac{dG_i(\theta-\theta_b\pm0.5\theta_{\delta i})}{d\theta}\right|_{\theta=\theta_s}=G_i'(\theta-\theta_b\pm0.5\theta_{\delta i})|_{\theta=\theta_s}\ .$$

Since the curves of identical diagrams within a linear area around the equal-signal direction are symmetrically placed, the slopes have different signs, and the processing results are the subtraction of the measured signal powers in different channels of the amplitude direction finders. The fifth and sixth terms are used to estimate the angular position of the radio source with the accuracy of the phase measurements. The basic operations are as follows: 1) the observations $u_5(t)$ and $u_6(t)$ must be passed through a filter whose parameters are matched to the complex envelope and frequency of the emitter signal; 2) the detection result at low frequency is multiplied by normalising factors $G_3(\theta_b)\left(j\pi f_0 dc^{-1}\right)K_{06}$; 3) the normalised amplitudes must be processed in a quadrature detector configured to measure the phase shift arising from the deviation of the radiation source from the equidistant zone. The processing results were converted to angles using the directional curve calculated on the right-hand side of (16). With the given parameters of antenna placement and orientation in the direction finder, the right-hand side of (16) is a function of angle θ_s and can be called the observation characteristic $\Psi(\theta_s)$ by its physical nature.

On the basis of the obtained optimal operations, it is advisable to develop a structural diagram of the radio direction finder and study its operation by simulation.

4. Development of the Block Diagram of the Optimal On-Board Radio Direction Finder and its Simulation Modelling

After analysing the algorithm (16), we developed a structural diagram of the radio direction finder, as shown in Fig. 3. The system consists of six antennas that receive electromagnetic waves and convert them into high-frequency signals. The signals from each antenna are transferred to an intermediate frequency and are coherently detected in filter $\dot{h}(t)$, which is tuned to the resonant frequency f_0 and complex amplitude $\dot{A}(t)$ of the radio source signal. After detection, the signals in the first, sec-

ISSN 1814-4225 (print)
ISSN 2663-2012 (online)

ond, third, and fourth channels are multiplied by the slope of the radiation patterns. If the measurements are made within the linear section of the patterns, the slope is a constant value. However, in general, the value $\left(dG_i\left(\theta-\theta_b\pm 0.5\theta_{\delta i}\right)\right)/d\theta\big|_{\theta=\theta_s}$ K_{0i} formation unit is a function of the angle θ_s, which must be estimated and constantly updated in the meter.

In the fifth and sixth channels, processing is more complicated because determining the phase shift in the received signals, which is caused by the deviation of the radiation source from the equal-signal direction. After coherent detection, the measurement results are multiplied by the coefficients K_{0i}, where i is the number of the corresponding channel, and the pre-calculated values

$$\cos(\pi f_0 d\cos(\theta_s-\theta_b)c^{-1})$$

and

$$\sin(\pi f_0 d\cos(\theta_s-\theta_b)c^{-1}).$$

In the channels of multiplication by function $\cos(\cdot)$, the obtained values must be additionally multiplied by the imaginary unit j. In the fifth channel, the quadrature components are subtracted, and in the sixth channel, they are added. The processing results in the sixth channel were subtracted from those in the fifth channel. The next operation in the developed structural diagram is multiplication by $\sin(\theta_s-\theta_b)$ to extract the voltage corresponding to the value of angle $\theta_s-\theta_b$. The estimation results in the fifth and sixth channels were multiplied by a normalising factor of $G_3(\theta_b)(\pi f_0 dc^{-1})$ and added to the measurements results in the first four channels. The resulting estimates were compared with the calculated values of the observational curve $\Psi(\theta_s)$ (right-hand side of equation (16)). After obtaining a non-zero value, the measured voltages are transmitted to the UAV control rudders to bring them into the radiation zone of the radio signal source. After correcting the direction, the process of measuring the angular position was repeated.

The structural scheme developed for the radio direction finder was simulated using the Simulink software by MathWorks in the DataFlow mode. The simulation model is shown in Fig. 4.

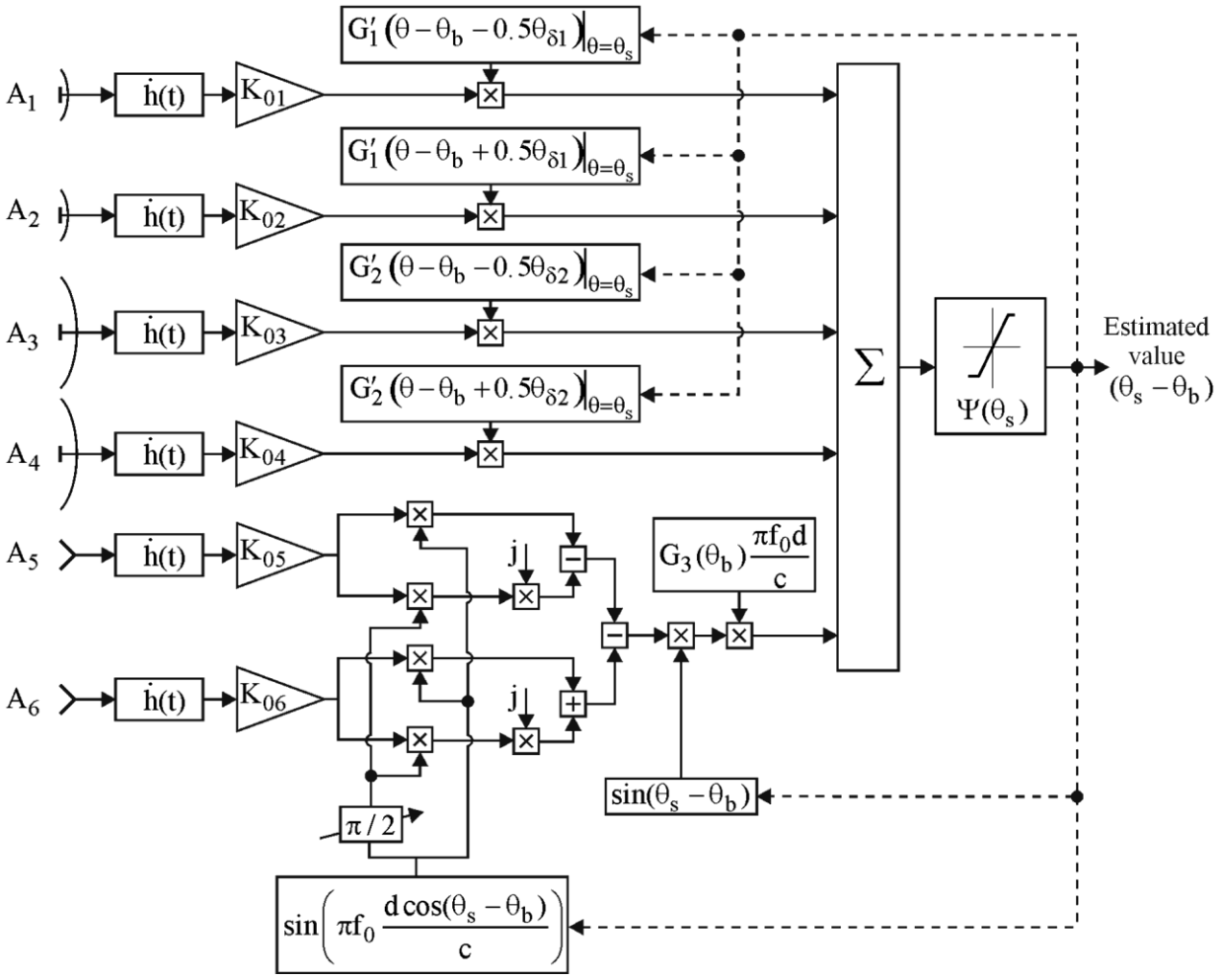

Fig. 3. Block diagram of the optimal six-antenna on-board radio direction finder

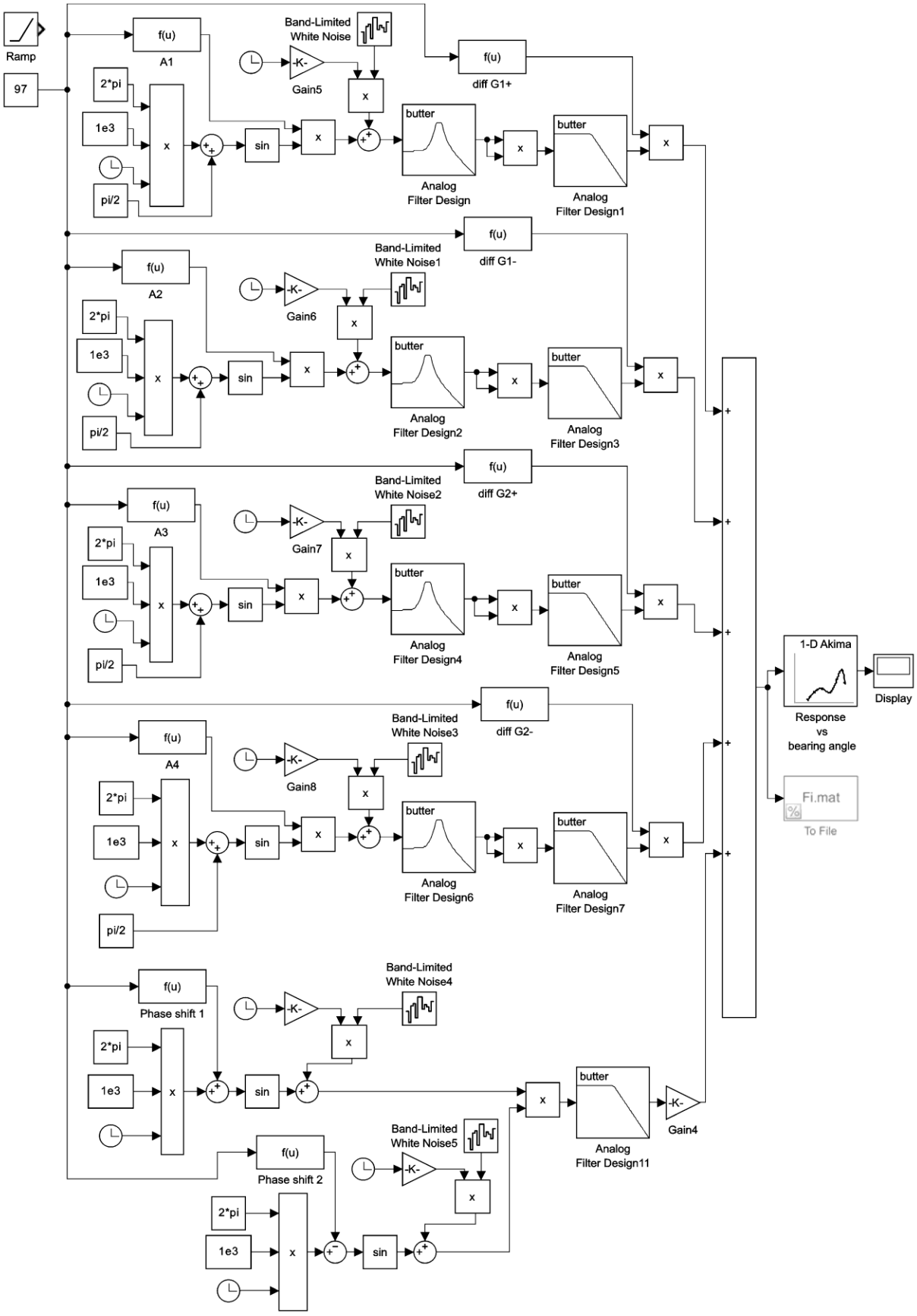

Fig. 4. Simulation model of high-precision on-board radar system direction of radio sources

ISSN 1814-4225 (print)
ISSN 2663-2012 (online)

Conventionally, a simulation model comprises six signal-processing channels. The input to each channel was a linearly time-varying angle from 0° to 180° or a fixed test value of $\theta_s = 97^\circ$. A linearly time-varying angle value is required to evaluate the observation characteristic $\Psi(\theta_s)$. Such measurements were performed under ideal conditions in the absence of internal noise.

Each channel was provided with Gaussian noise with the same statistical characteristics and limited spectrum. Such noises are generated by the "Band-Limited White Noise" block, which generates Gaussian noise with a unit variance, and the "Clock" and "Gain" blocks. The latter are used to generate a time-varying noise variance, which is used to estimate the direction-finding error. The time-varying variance of the internal noise was multiplied by the noise in units. All parameters of the blocks in each channel were configured in the same way, but the "Seed" parameter in "Band-Limited White Noise" has different values to generate uncorrelated sequences between channels.

Let us consider in more detail the channels of signal formation and processing. Each channel has a set of blocks for generating a carrier oscillation in the form of a function $\cos(2\pi f_0 t)$, including a constant block 2π, a 1 kHz constant value generator, a time generator t, a phase shift generator $\pi/2$, and a trigonometric function block $\sin(2\pi f_0 t)$. The fifth and sixth channels (counting from top to bottom) do not have a fixed shift $\pi/2$, but add a phase shift caused by the deviation of the radio signal radiation source from the equal-signal direction to the trigonometric function. The first two channels describe the signals in the amplitude direction finder with wide-directional antennas, the third and fourth channels describe the signals in the amplitude direction finder with narrow-directional antennas, and the fifth and sixth channels describe the phase direction finder.

The radiation pattern of the first four antennas is implemented in blocks A1, A2, A3, A4 in the form of a function

$$G_i\left(\theta-\theta_b\pm\frac{\theta_{\delta i}}{2}\right)=a_i e^{-\frac{\left(\theta-\theta_b\pm\frac{\theta_{\delta i}}{2}\right)^2}{2\sigma_i^2}}$$

where $i=\overline{1,2}$; $\theta_b = 90^\circ$ is equal-signal direction, where in the first two antennas $\sigma_1 = 40$, $0.5\theta_{\delta 1} = 40$, $a_1 = 20$. The next two narrowly directed antennas have parameters $\sigma_2 = 5$, $0.5\theta_{\delta 2} = 5$, $a_2 = 4$.

The values of the selected test angle or linearly variable angle values are passed through blocks A1, A2, A3, and A4, and are then multiplied by the high-frequency received signal. In this simulation model, the centre frequency is set to 1 kHz for simplicity, while the real values are in the units and tens of GHz.

The useful signals generated by the amplitude and phase direction finders with the angular position information are added to the internal noise of the receivers. The following blocks are dedicated to signal processing and estimating the bearing to the radio source. The first processing block is an analogue filter tuned to the resonant frequency of the signal. This filter acts as a matched filter with an impulse response of $\dot{h}(t)$. The next operation in the first four channels is the quadratic detection of the signal amplitude and the averaging of the received oscillations in the low-pass filter, which implements the integration operation in (16). To extract useful information from the obtained amplitudes in the first four channels, the oscillations after the low-pass filter were multiplied by the derivatives of the radiation patterns of each channel. Such amplitudes are implemented as derivatives of the radiation patterns in the blocks diff G1+ (first channel), diff G1- (second channel), diff G2+ (third channel) and diff G2- (fourth channel). The results of the multiplication are added to the adder of all channels.

The common adder also receives the voltage from the phase finder implemented in the fifth and sixth channels. Useful signals mixed with noise are multiplied and filtered using a low-pass filter. Because of these operations, the uncorrelated internal noise is suppressed, and a voltage proportional to the phase difference between channels is estimated. The voltage varies according to the sine law depending on the deviation of the signal from the equal-signal zone. The Gain4 amplifier corrected the effect on the overall measurement of the phase finder.

The results of the summation of all the amplitudes at the first stage of the model were written to the Fi.mat file with zero values of the internal noise variance (Gain5, Gain6, Gain7, Gain8, Gain9, Gain10). The resulting file entries represent estimates of the observation characteristic $\Psi(\theta_s)$. Fig. 5 shows $\Psi(\theta_s)$ for four types of direction finders. Fig. 5(a) shows the observation characteristics of an amplitude direction finder with wide-directional antennas, Fig. 5(b) shows the observation characteristics of an amplitude direction finder with narrow-directional antennas, Fig. 5(c) shows the observation characteristics of a combination of the first two direction finders. The curve on Fig. 5(d) shows the observation characteristics of the amplitude direction finders and the phase direction finder when they work in combination.

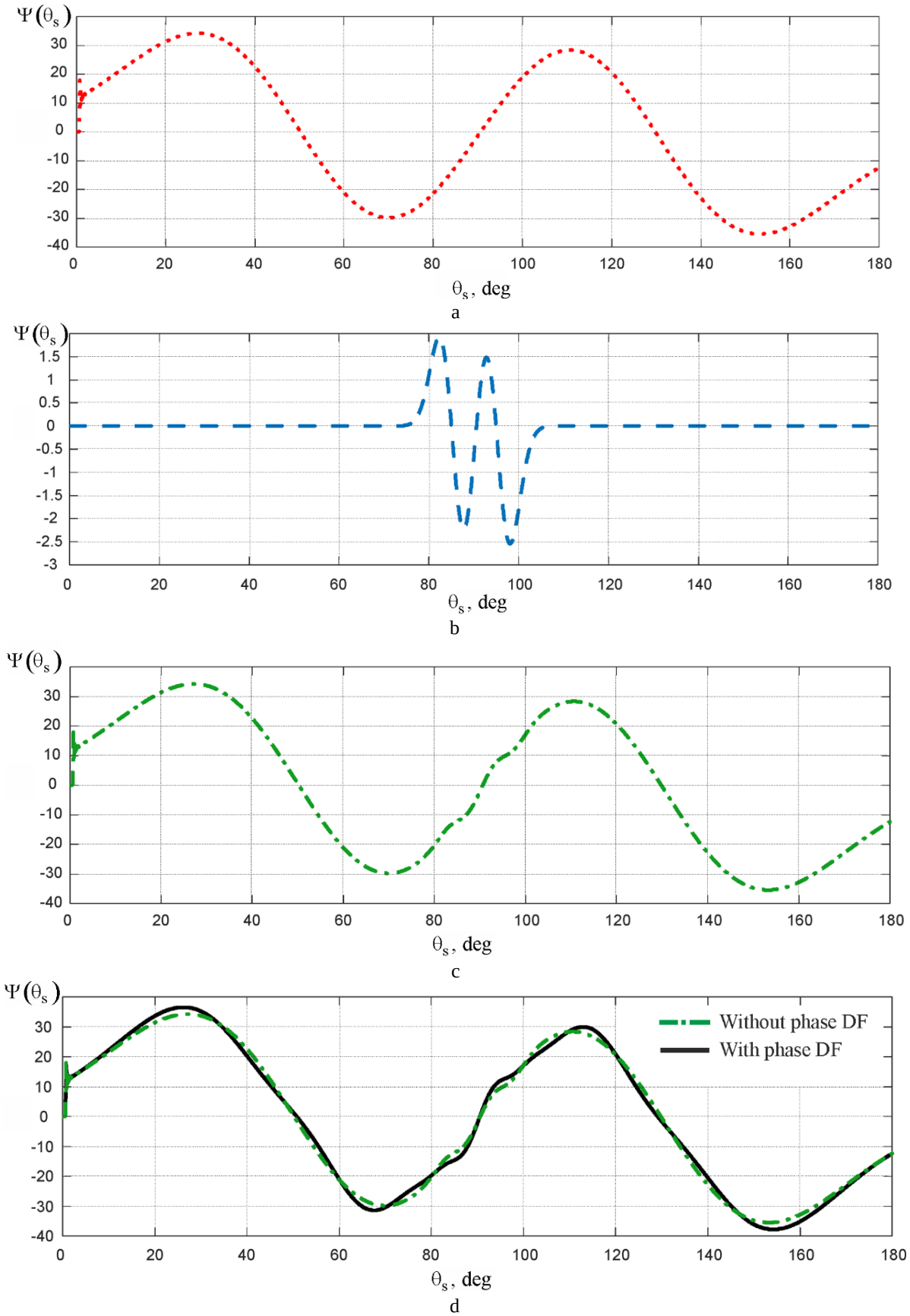

Fig. 5. Observation characteristics of different types of direction finders: a) is for an amplitude direction finder with narrowly directed antennas; b) is for an amplitude direction finder with wide directional antennas; c) is for the combination of two amplitude direction finders; d) is for a combination of two amplitude and phase direction finders

ISSN 1814-4225 (print)
ISSN 2663-2012 (online)

From the obtained observation characteristics, it follows that the combined direction finder of two amplitudes and one phase direction finder has the widest range of unambiguous measurements because it has the widest range around the equidistant direction, where the curve increases monotonically. The disadvantages include different values of the steepness of the discrimination curve in unambiguous measurements, which have different accuracy values for different angles. At the same time, it can be seen that accuracy increases with approximation to the equal-signal direction.

To evaluate the accuracy, we measured the angle of 97° at different dispersions of the internal noise of the receivers. The results of the simulated measurements are shown in Fig. 6.

The ordinate axis shows the measured angle, and the abscissa axis shows the change in the signal-to-noise ratio in dB. At the beginning of the first graph, there are measurement pulsations, which is a transient process in the analog filters used in the simulation model. At the end of the first curve, significant measurement distortions can be observed due to the high dispersion of internal noise. The second graph shows the most typical range of the signal-to-noise ratios in the radar. At a value greater than 13 dB, only a shift of 0.5812° from the specified value is observed, and the variance of the spread is several orders of magnitude less than this value. As the signal-to-noise ratio decreases, the estimated shift and variance of the values increase.

By analysing the results of the simulation modelling, we can conclude that the proposed method is efficient and that the estimated angular positions are generally consistent with known measurements in the presence of interference.

Next, the theoretical methods and DataFlow simulations need to be confirmed experimentally. To achieve this, it is necessary to design and manufacture a set of receiving antennas and implement a receiving radio path for both amplitude and phase direction finders. To simplify the development, the layout of the direction-finding system was developed for the 2.4-2.5 GHz frequency band. According to Ukrainian regulations, this band can be used by industrial, scientific, medical, and household radio-emitting devices if there is no interference from radio services operating in these frequency bands. Also, the radio element base was extremely developed for this frequency band, which greatly simplified the final system development.

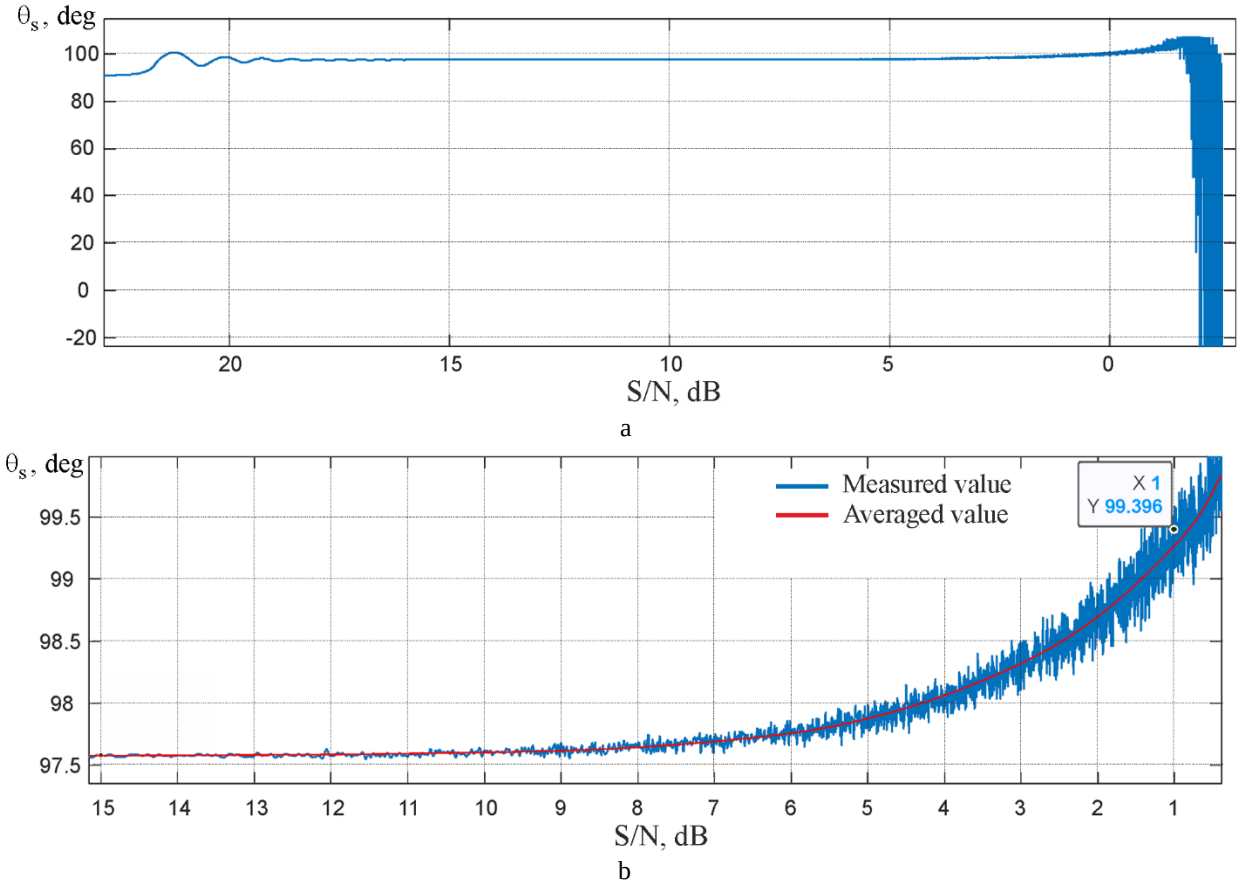

Fig. 6. Measurement of the fixed value of angle $\theta_s = 97^\circ$ depending on the signal-to-noise ratio:
a) has the range of values from 28 to 0.5 dB in power; b is an enlarged section of the most typical case of signal-to-noise ratio in radar

5. Antenna System of the Radio Direction Finder

When choosing a specific type of antenna in system implementation, it is necessary to ensure that their impact on the aerodynamic characteristics of the carrier is minimized. For an on-board system, antennas can be implemented in two main ways: planarly on printed circuit boards or using wires [29, 30].

The main advantages of planar design are the high repeatability of the product and the ability to quickly manufacture a large series. However, planar antennas with narrow radiation patterns usually take up a significant area on printed circuit boards, which can negatively affect the aerodynamics of the carrier, making them much more difficult to manufacture on their own. At the same time, wire antennas have a smaller impact on the aerodynamics of aircraft because they have a smaller area. Also, their manufacture does not require specialised equipment. Therefore, a wire implementation was selected for the development of direction-finder model antennas.

According to the geometry shown in Fig. 2, the antenna system of the direction-finding complex includes two omnidirectional antennas for phase measurements, as well as two wide- and two narrow-directional antennas for amplitude measurements.

The simplest to implement are the omnidirectional antennas of the phase-direction finding method. Taking into account the requirement to receive signals over a wide range of angles and to simplify the direction-finding system as a whole, it is advisable to choose dipole or monopole antennas [31]. Their general schemes are illustrated in Figure 6. Thus, in general, a dipole antenna consists of two symmetrical quarter-wave conductor segments. The output signal from the two poles is fed to the receiver. A monopole antenna usually consists of a single quarter-wave conductor and a ground plane to which the receiver is connected. The geometry of the ground plane is usually chosen to match the antenna and receiver in terms of wave impedance [32].

It should be noted that in Fig. 6, λ_{ant} is the wavelength with the velocity factor that occurs when a radio wave propagates in a nonvacuum and not in an ideal conductor.

To accelerate the development of the phase-direction finder, factory-made monopole antennas with SMA connectors were used as the antennas, as shown in Fig. 7(a). Fig. 7(b) also shows the standing wave ratio (SWR) of the available antennas, as measured by a calibrated R&S ZNL20 vector network analyser.

As shown in Fig. 7(b), in the 2.4-2.5 GHz frequency band, the VSWR of the existing antenna is in the range of 1.974-1.722. This value is sufficient for the receiving antenna and confirms the feasibility of its use for phase-direction finding at selected frequencies.

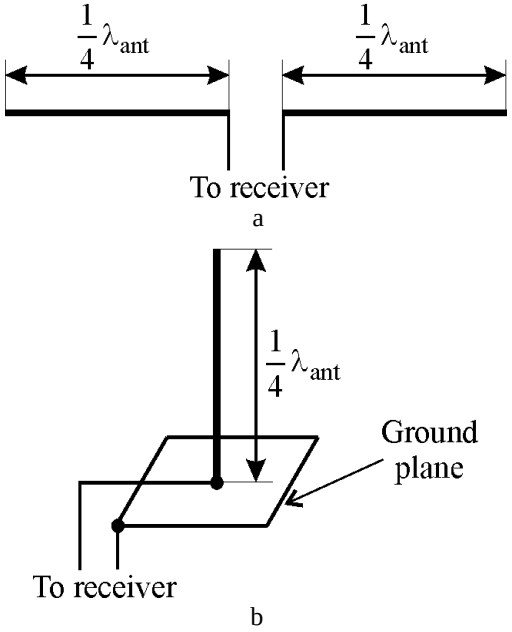

Fig. 6. General geometries of dipole (a) and monopole (b) antennas

a

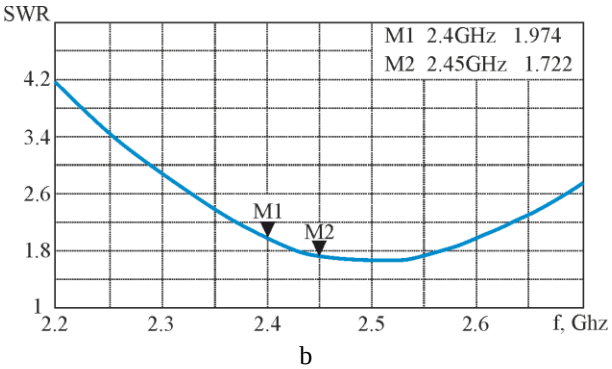

b

Fig. 7. The used monopole antenna (a) and its measured SWR (b)

To implement the amplitude direction finding method, it is necessary to use more complex antennas than in the phase method. This is because the measurement results for such direction finders directly depend on the shapes of the radiation patterns of the antennas used. In this case, it is advisable to choose antennas

ISSN 1814-4225 (print)
ISSN 2663-2012 (online)

whose beamwidths can be changed, for example, during the manufacturing stage. At the same time, it is advisable to choose an antenna with a simple geometry, which is easy to calculate and manufacture, and which in the future will not significantly affect the aerodynamic characteristics of the direction-finder carrier. A collinear antenna array is a possible variant of such an array [33]. Such arrays usually consist of a set of dipole elements mounted along a common axis that are connected in series by phase-shifting lines. In general, these lines should result in a 180° phase shift of the radio wave between adjacent antenna elements. The total width of the radiation pattern of a collinear antenna array is determined by the number of elementary dipoles in the array. Increasing the number of elements in the antenna narrows its radiation pattern.

One of the most common collinear antenna arrays is the Franklin and Super J-pole antenna [34, 35]. The general principles of the antenna construction are similar, and the main difference lies in the feeding points. Fig. 8 shows the general geometry of the Franklin antenna, and Fig. 9 shows the Super J-Pole antenna.

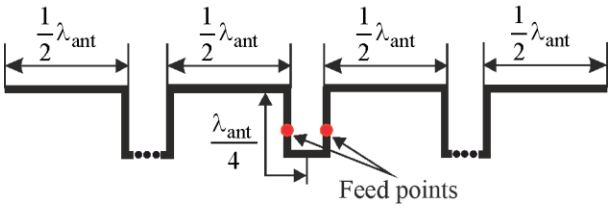

Fig. 8. General geometry of the Franklin antenna

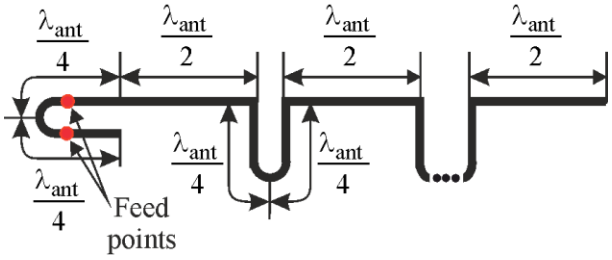

Fig. 9. General geometry of the Super J-Pole antenna

According to the geometries of the diagrams, the Franklin antenna is connected to the central phase-shifting element. The antenna is symmetrical with respect to this element, and the feed points are usually selected experimentally under the condition of the best matching, i.e., the minimum standing-wave coefficient at the operating frequency. The Super J-Pole antenna is connected to one of its ends. To match the antenna, a matching element is added on which the feed points are selected. As in the case of the Franklin antenna, the feed points were searched with a minimum standing wave ratio. These types of antennas also differ in terms of the shape of the phase-shifting elements. In Franklin antennas, they remain in a Π-shape, while in Super J-Pole antennas, they are bent into a ring.

The reviewed antennas have similar characteristics, and it is advisable to choose a particular one based on the convenience of connection. In our case, it is more convenient to connect the antenna from the edge, which in the future will reduce the required cable length between the antenna and the radio elements, which should be placed in the fuselage of the carrier. Therefore, Super J-Pole antennas were selected for the implementation of amplitude direction finders.

To implement antennas with a wide radiation pattern, we decided to use a Super J-Pole with three elements. To determine the geometric dimensions of the antenna, it is necessary to calculate λ_{ant}, which can be represented by the following formula:

$$\lambda_{ant} = \frac{c}{f_c} k_p, \qquad (12)$$

where f_c is the central operating frequency of the antenna; k_p is the velocity factor.

Because the antenna will be made of copper wire with a diameter of 1.8 mm, the coefficient k_p is quite difficult to determine. However, radio amateurs usually choose it at the range of 0.9-0.97 when making such antennas. For calculations, we assume that $k_p = 0.95$. Then, at a central frequency of 2.45 GHz, λ_{ant} is approximately equal to 11.6 mm. Considering the obtained value and the ratio shown in Fig. 9, a 3-element antenna was manufactured, and a general view of the antenna is shown in Fig. 10(a). The feed point of the antenna was determined using an R&S ZNL20 vector network analyzer. The vector network analyzer also measured the frequency dependence of the standing-wave coefficient. The results are shown in Fig. 10(b).

As can be seen in Figure 10(a), the SWR of the developed antenna in the operating frequency range is 2.239 or less. This value is acceptable for a receiving antenna.

Next, a pair of 9-element Super J-Pole antennas with a narrow radiation pattern was manufactured. A photo of an antenna and its measured standing wave ratio are shown in Fig. 11.

According to the graph in Figure 11(b), the standing wave ratio of the 9-element antenna in the operating frequency range did not exceed 1.4, which is a good result.

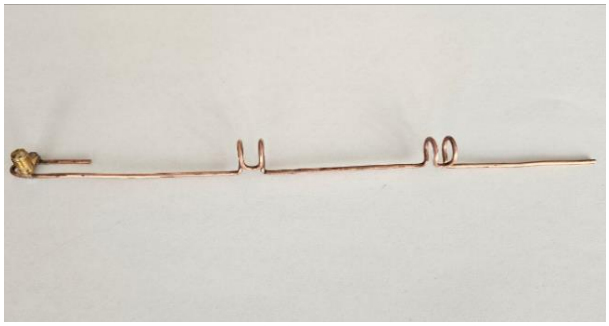

a

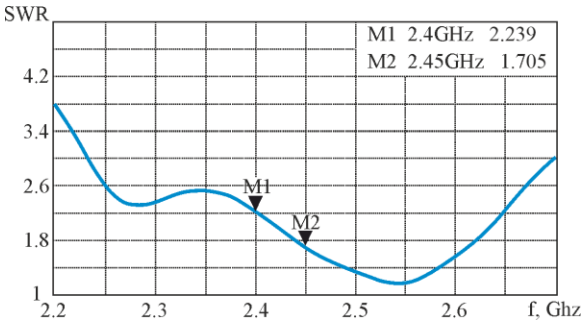

b

Fig. 10. The constructed 3-element Super J-Pole antenna (a) and its measured standing wave ratio (b)

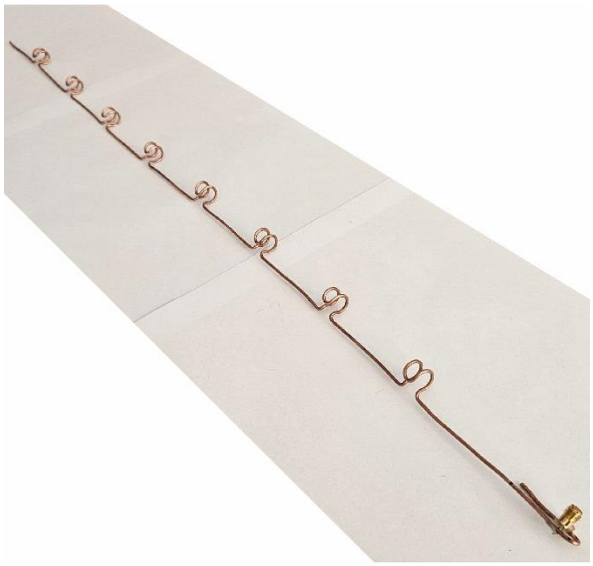

a

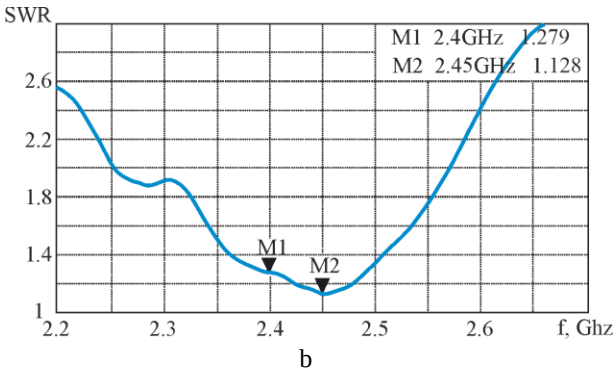

b

Fig. 11. The constructed 9-element Super J-Pole antenna (a) and its measured standing wave ratio (b)

Thus, a set of antennas necessary for the creation of the proposed experimental direction-finding complex was selected and constructed. Next, it is necessary to create measurement radio paths to which the antennas will be connected.

6. Selection of Radio Path Components of the Direction Finding System

To implement the phase-direction finding algorithm, it is necessary to calculate the phase difference of the signals received by the spaced omnidirectional antennas. In practice, phase detectors are used for this purpose, and the general structure of the phase-direction finder radio path is illustrated in Fig. 12.

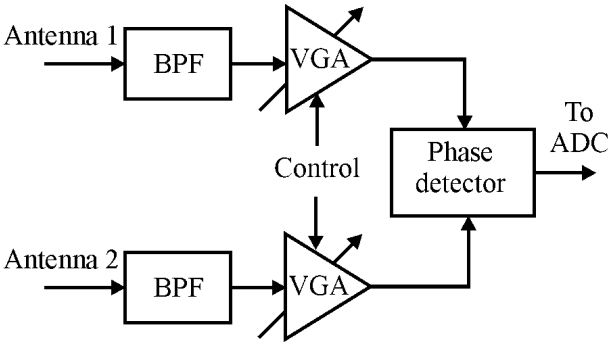

Fig. 12. General structural diagram of the radio path of the phase direction finder

According to the diagram in Figure 12, the signals from the outputs of the omnidirectional antennas are fed to the inputs of the bandpass filters (BPF). The filtered oscillations are amplified in variable gain amplifiers (VGA) and passed to a phase detector. The phase detector generates a voltage proportional to the phase difference of the input signals. The voltage is digitised by an analogue-to-digital converter (ADC) and further processed by a computing unit. A band-pass filter at the input must isolate the working-frequency band and reduce the influence of out-of-band noise on the measurement. VGA must adjust the signal power at the input of the phase detector, which extends the operating range of direction detection. When the direction finding system is far from the transmitter, the gain is high. When getting closer to the transmitter, the gain gradually decreases, and the signal strength at the detector input is maintained within its operating range.

In our case, during the experiment, the direction finder receives a signal from a transmitter at a distance of several tens of metres. This is due to the current impossibility of conducting measurements over long distances. In addition, measurements will occur in a place with a small amount of noise in the working band of the

ISSN 1814-4225 (print)
ISSN 2663-2012 (online)

direction finder. In this case, the bandpass filters and VGA in Fig. 12 can be ignored. The antennas can be connected directly to the phase detector, whose technical implementation must be chosen.

In our case, during the experiment, the direction finder receives a signal from a transmitter at a distance of several tens of metres. This is due to the current impossibility of conducting measurements over long distances. In addition, the measurements take will be placed in a location with low noise in the operating frequency band of the direction finder. In this case, the bandpass filters and VGA in Fig. 12 can be ignored. The antennas can be connected directly to the phase detector, whose technical implementation must be chosen.

In general, there are two main ways to implement a phase detector: using specialized phase detector chips or using high-frequency signal multipliers with subsequent low-pass filtering. An example of a phase detector chip is the AD8302 from Analog Devices, which has an operating frequency band of up to 2.7 GHz [36]. A detection variant with multiplication of high-frequency signals can be implemented on an ADL5391 chip of the same company [37]. However, the operating frequency range of this chip is limited to 2 GHz, which makes it impossible to use it in selected frequency bands. A possible solution to this problem is to shift the high-frequency signal to an intermediate frequency before detection, but this will complicate the system. Therefore, to implement the phase-direction finding method in the proposed system, the AD8302 phase detector was chosen, and the module based on which is shown in Fig. 13.

When implementing a phase detector on an ADL5391 chip, it is necessary to consider the dependence of its output voltage on the phase difference of the signals at the inputs. This dependence is illustrated in Fig. 14.

As can be seen, at a phase difference of 0° at the detector inputs, the output voltage has a maximum value and decreases regardless of whether the phase difference decreases or increases. This leads to measuring ambiguity and does not allow us to determine the direction to the radio source. To eliminate this problem, it is advisable to shift the operating point of the detector to the centre of one of the linear sections, i.e., to the point of phase difference 90° or -90° marked on the graph. In our case, this is achieved by increasing the length of the cable between the antenna and detector channel A by a length equal to one-fourth of the wavelength at the central operating frequency, taking into account the shortening factor.

It is also necessary to implement radio paths for each amplitude direction finding channel. In general, the structural diagram of such paths can be represented as shown in Fig. 15.

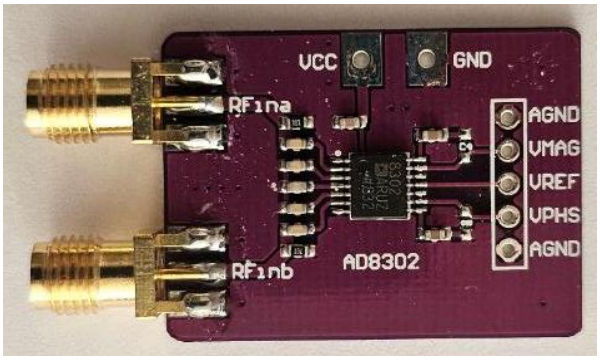

Fig. 13. Used module based on ADL5391

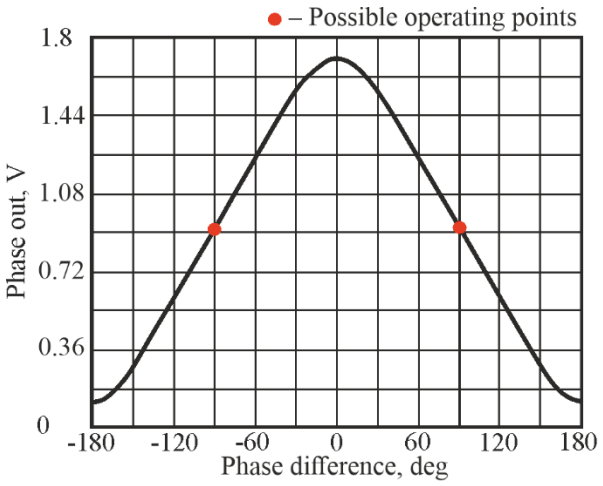

Fig. 14. Dependence of the AD8302 output voltage on the phase difference of the input signals [36]

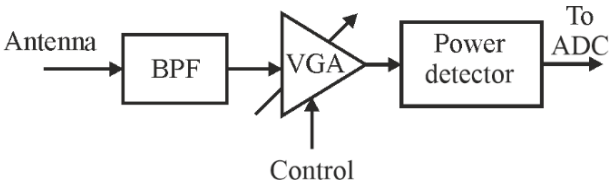

Fig. 15. General structural diagram of the radio path of the amplitude direction finder channel

As shown in Fig. 15, the signal from the antenna output is fed to a bandpass filter tuned to the operating-frequency band of the system. The received signal is amplified in the VGA and detected by the power detector. The output of the detector generates a voltage proportional to the received signal power, which is then digitised and processed in a computing device. As observed for phase direction, BPF reduces the impact of out-of-band interference on the measurement results. Using VGA, the signal power at the detector input is maintained within the dynamic range, which significantly increases the operating range of the radio source direction detection.

As noted earlier, the experimental study will be conducted at a short distance with low interference. Therefore, the BPF and VGA in the experimental layout can be excluded and limited to directly connecting the antenna to the detector input. The existing quadratic detector AD8361 [38] was used as the detector. The board made for the experiment is shown in Fig. 16. Such boards were made for each amplitude direction finding channel.

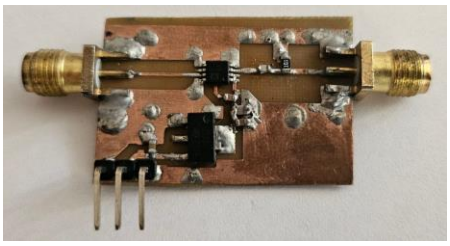

Fig. 16. Designed board based on AD8361

7. Experimental Studies of the Direction Finding System and Results Discussion

Based on the developed components and antennas, an experimental sample of the proposed direction-finding complex was assembled, and a general view of the result is shown in Fig. 17.

All antennas were interconnected with the corresponding detectors. The antenna holders and cases were printed on a 3D printer with PETG plastic, which minimises changes in the parameters of the antenna system. The phase direction finder antennas were installed at a distance of 12 cm. The outputs of the detectors were connected to an AD7608 ADC as part of the signal control and digitisation system [39]. The basis of the signal control and digitisation system was the ARTY S7-50 development board based on the AMD Spartan-7 FPGA. The control board processes signal from the ADC module, transmits them to a personal computer, and controls the automatic rotary platform.

Next, we conducted an experimental study of the direction finder. For this purpose, a direction finder was installed in an open space, and a transmitter tuned to a frequency of 2.45 GHz was placed at a distance of 25 m from the transmitter. A 1W video transmitter module was used as the radio signal source. The experiment's direction finder and transmitter positions are shown in Fig. 18.

During the experiment, the direction finding system was rotated in the range of angles from -90° to 90° relative to the direction to the transmitter. In parallel, every 0.25° the voltage values from the outputs of the system's detectors were digitised and stored. Previously, the angular positions of the antennas were adjusted so that their radiation patterns at 0.5 of the maximum power level intersected with the direction of the transmitter 0°.

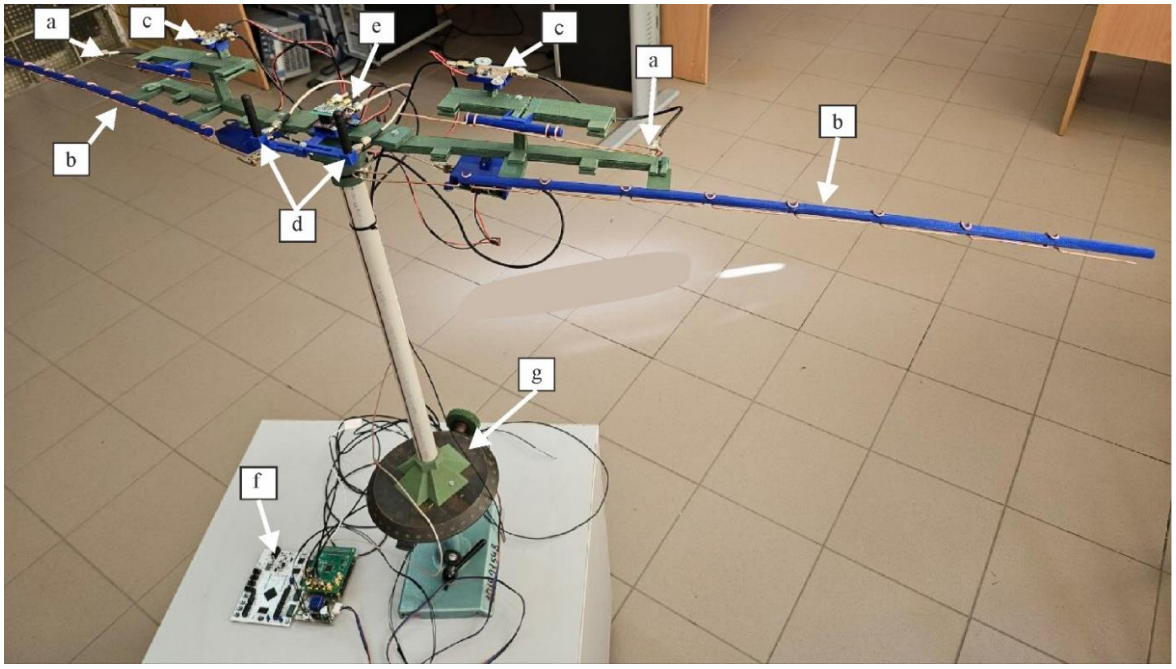

Fig. 17. An experimental model of the direction finding complex has been developed: a) are antennas with a wide radiation pattern; b) are antennas with narrow radiation patterns; c) are AD8361 power detectors; d) are omnidirectional antennas; e) is phase detector based on ADL5391; f) is control and signal digitisation system; g) is automatic rotary platform

ISSN 1814-4225 (print)
ISSN 2663-2012 (online)

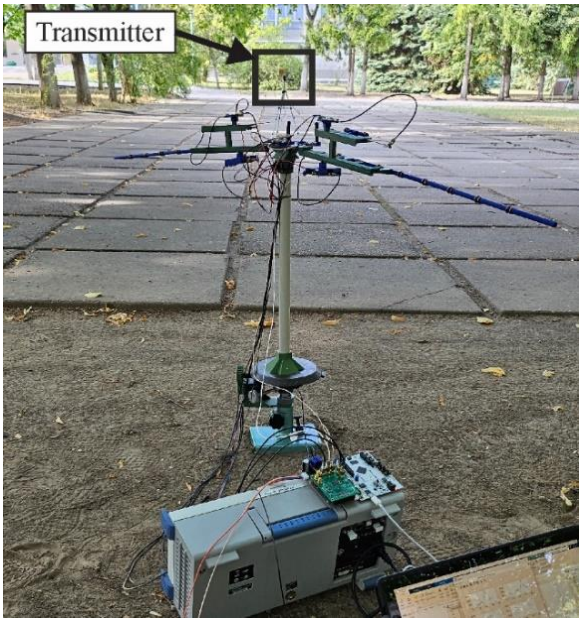

Fig. 18. Position of the transmitter and direction finder during measurements

As a result, the voltage-angle dependences were obtained, where for the amplitude channels correspond to the parameters of the antenna radiation patterns, and for the phase detector, the direction finding characteristic shifted to the positive voltage range. The measurement results from the outputs of the power detectors are shown in Fig. 19, and those from the output of the phase detector are shown in Fig. 20. To simplify the analysis of the results, the graphs were normalised.

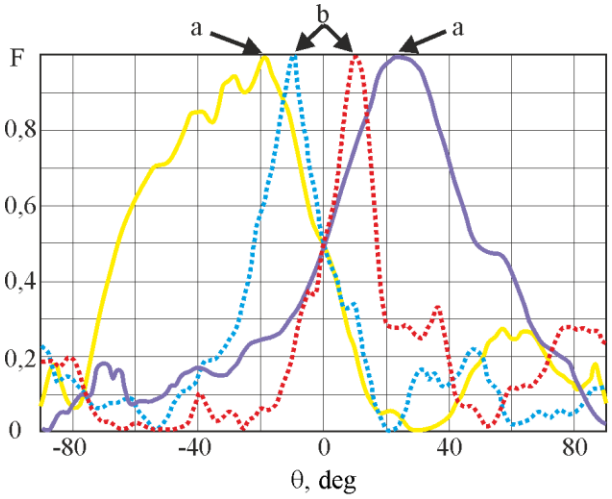

Fig. 19. Directional patterns of antennas with 3 (a) and 9 (b) elements

In accordance with Fig. 19, 3-element antennas at level 0.5 have radiation patterns widths of 60° and 50°. The radiation patterns of 9-element antennas are 17° and 22°. Differences in the radiation patterns of similar antennas may be due to their manual manufacturing process and the possible inaccuracies that may arise in this case.

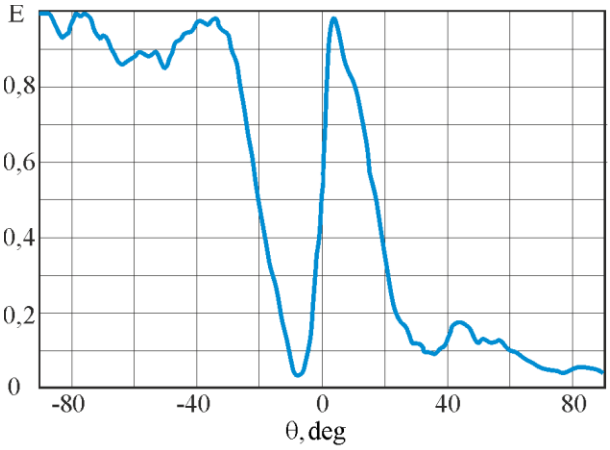

Fig. 20. Normalised voltage at the output of the phase detector

From the obtained characteristics of the phase-direction finder in Fig. 20, it is possible to determine its range of unambiguous measurements, which is defined by the angular positions of the first extremes relative to the centre of the curve. As a result, the range of unambiguous measurements is 10.2°. It should also be noted that the data presented in Fig. 20 are usually preliminary. Their use for determining the angular direction to the radio source requires additional processing, namely, shifting the normalised curve by 0.5 units to the negative region and scaling it by a factor of 2. Typically, equivalent operations are performed at the direction finder calibration stage.

Next, we obtain separate observation characteristics for amplitude direction finders with narrow-directional antennas and antennas with a wide radiation pattern. According to equation (11) and the diagram in Fig. 3, the value at the detector output must be multiplied by the derivative of the radiation pattern. In practice, it is extremely difficult to consider the type of antenna pattern at each measurement moment because the antenna pattern can change under the influence of surrounding objects. In this case, it is advisable to consider not the full value of the derivative but its sign within the operating range of angles, i.e., between the point of maximum RP and the point of intersection of the radiation patterns of two antennas of the same type. In this case, one derivative has a positive value, and the other has a negative value. Then, processing in the amplitude direction finder with the same type of antenna can be reduced to the following form:

$$u_{out}(t,\theta_s) = K_{01,03}\int_T u_{1,3}(t)\dot{h}(t)dt - \\ -K_{02,04}\int_T u_{2,4}(t)\dot{h}(t)dt. \qquad (13)$$

According to equation (13), in simplified processing, it is sufficient to determine the power of the radio signals received by a pair of antennas, multiply the obtained values by the gain coefficients of the corresponding channels, and subtract the result. This, except for the multiplication by coefficients, corresponds to classical signal processing in two-antenna amplitude direction finders. Considering expression (13) and the need for additional processing in the phase direction finder, a graph with the individual discriminative characteristics of each direction finder available in the complex was obtained. The results are shown in Fig. 21.

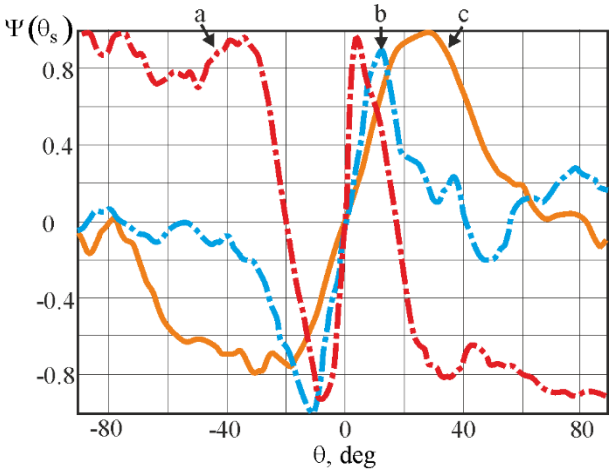

Fig. 21. Obtained observation characteristics:
a) is for the phase direction finder;
b) is for the amplitude direction finder
with 9-element antennas; c) is for the amplitude
direction finder with 3-element antennas

According to the obtained observation characteristics, the range of unambiguous measurements obtained by the developed dual-antenna direction finder with antennas having a wide radiation pattern is 46.5°. For narrowly directed antennas, the range of unambiguous measurements is 23°. Another important parameter of the obtained discrimination characteristics is the slope of the discrimination characteristics, which determines the accuracy of the direction finder. We define this characteristic as the ratio of the increment of the discrimination characteristic normalised value E to the increment of the observation angle θ. Let us determine the steepness in the area of angles from -2° to 2°, which is close to the desired angular direction to the radio source 0°.

The steepness of the observation characteristic of the direction finder with 3-element antennas is 0.045 units/deg, while for the case of a 9-element antenna it is 0.093 units/deg. The value of 0.28 units/deg. was obtained for the phase direction finder.

Next, we processed the measurements in accordance with the mathematical model (11) proposed in this paper, which involves summing the measurement results by the factors K_{0i}. These factors are generally selected separately for each of the measurement channels, as shown in the block diagram in Fig. 3. However, to simplify the calculations and the system as a whole, it is advisable to choose the same factors in each system, i.e. $K_{01} = K_{02}$, $K_{03} = K_{04}$, $K_{05} = K_{06}$. Currently, there are no optimal methods for selecting these factors; thus, they are chosen heuristically for the following reasons. The amplitude direction finder with 3-element antennas provides unambiguous measurements over a wide range of angles, so the factors K_{01}, K_{02} will have the highest value as the measurement with the highest confidence level. The factors of K_{03}, K_{04} will have smaller values because the amplitude direction finder with a 9-element antenna provides a smaller range of unambiguous measurements and the factors K_{05}, K_{06} of phase direction finder will be the smallest.

For convenience, we fix the coefficients of the phase direction finder $K_{05} = K_{06} = 1$, and change only the coefficients of the amplitude-direction finders. To verify the feasibility of using the phase-direction finder, we constructed the observation characteristics for cases in which phase measurements were excluded from the calculations ($K_{05,}K_{06} = 0$). Some obtained graphs of the normalized observation characteristics of the direction-finding complex are shown in Fig. 22. Table 1 lists the parameters of the direction-finding complex (range of unambiguous measurement (RUM) and observation characteristic steepness (OCS)) for a larger number of factor K_{0i} possible values.

Analysing the results shown in Figure 22 and Table 1, we confirmed the overall performance of the experimental model for the direction finding complex and the synthesized signal processing algorithm. For example, at $K_{1,2} = 10$, $K_{3,4} = 5$ and $K_{5,6} = 5$, the range of angles in which the unambiguous determination of the direction to the radio source is ensured is 29.4°. This value is higher than the individual capabilities of a phase-direction and amplitude-direction finders with a 9-element antenna. This was achieved using an amplitude direction finder with 3-element antennas with wide radiation patterns. At the same time, the steepness of the observation characteristic in the range of angles from -2° to 2° was 0.1 unit/deg. Amplitude direction finders without a phase system are not capable of providing such direction-finding accuracy.

As shown in Table 1, if the measurements of the amplitude direction finder with 9-element antennas ($K_{3,4} = 0$) or the phase direction finder ($K_{5,6} = 0$) are

ISSN 1814-4225 (print)
ISSN 2663-2012 (online)

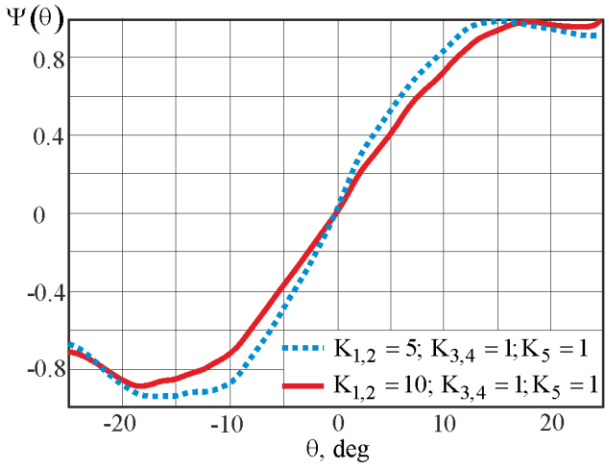

a

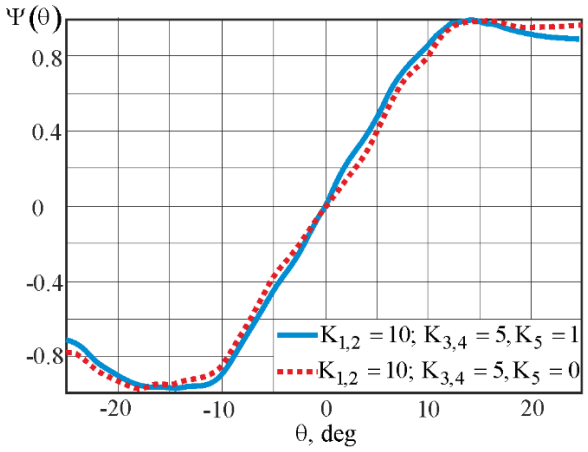

b

Fig. 22. Graphs of the observation characteristics of the direction finding complex: a) at different gain in an amplitude direction finder with a 3-element antenna; b) with and without a phase direction finder

Table 1

Parameters of the observation characteristic of the direction finding complex at different values of the factors

Factor values			RUM, deg.	OCS, units/deg.
$K_{1,2}$	$K_{3,4}$	$K_{5,6}$		
5	1	1	29.5°	0.12
10	1	1	36°	0.09
10	5	1	29.4°	0.1
10	5	0	29.5°	0.08
10	0	1	31.2°	0.08
20	1	1	43.3°	0.06
20	5	1	32.8°	0.08
20	10	1	28.3°	0.09
20	15	1	24.2°	0.1

excluded from the processing, the measurement accuracy decreases by 20% to 0.08 units/deg. At the same time, the operating range of the angles was not significantly changed. This indicates the expediency of using three systems at once, which complement each other and form a complex.

At the same time, the proposed direction finding complex and mathematical model of the signal-processing algorithm (11) at this stage of work have drawbacks. For example, it is impossible to specify the most effective approach for determining the factors of amplification K_{0i}, which are introduced into each of the amplitude and phase direction finders channels. At present, this problem is most expediently solved heuristically, i.e., by selecting such values K_{0i} that will provide the best characteristics of a particular system for solving the current problem. In addition, according to the obtained results, although the proposed direction finding complex provides better parameters than individual direction finders, it still requires a compromise between the direction finding accuracy and the range of angles in which unambiguous measurements are provided. An interesting way to address these shortcomings is to implement an adaptive direction finding system in which the coefficients K_{0i} will be determined automatically in real time. This will make it possible to adjust the system to the widest range of unambiguous measurement angles or to increase the direction-finding accuracy, depending on the direction-finding results of the radio source. However, this approach requires additional research to be conducted in the future. In addition, the on-board implementation of the direction-finding system requires a study of the influence of external radiation on the measurement results and automation of wire antenna manufacturing [40, 41].

7. Conclusions

When designing simple direction-finding systems, engineers usually need to find a compromise between the accuracy of determining the angle to the radio source and the range of angles in which measurements can be performed unambiguously. This paper proposes a possible solution to this problem. This involves the creation of a complex that includes two amplitude direction finders and one phase direction finder. The amplitude direction finder consists of antennas with wide radiation patterns, which provides several unambiguous measurement angles at low accuracy. The second amplitude direction finder contains narrowly directed antennas, which reduces the range of unambiguous measurement angles but increases accuracy. The phase-direction finder exhibits the best accuracy, but it is provided only over a narrow range of angles. The implementation of such a direction-finding complex provides high measurement accuracy over various angles.

To combine the measurement results of the three systems, a mathematical model (11) of the optimal signal-processing algorithm was synthesised using the maximum-likelihood method. According to the mathematical model, optimal signal processing involves summarising the measurement results of each individual direction finder, considering factors 1, which are generally determined separately for each channel. The resulting processing algorithm also considers the shapes of the radiation patterns of each antenna and the quadrature demodulation of the signals received by the phase-direction finder.

On the basis of the synthesised mathematical model, a structural diagram of the proposed direction-finding complex and its simulation model were developed. As a result of simulation modelling, the efficiency of the proposed method, the possibility of achieving new quality criteria in the proposed complex, and the general conformity of the obtained angular position estimates to known cases of measurements in the presence of interference were confirmed.

The efficiency of the proposed approach was experimentally confirmed. For this purpose, antennas of individual direction finders, measuring radio components, and a control and signal processing system were developed, which were assembled into a direction-finding complex. Because of experimental studies on the direction-finding system, its overall performance and efficiency in terms of the proposed approach to system implementation were confirmed. The proposed signal processing allows us to achieve an extended range of unambiguous measurement angles with increased direction finding accuracy compared to individual systems.

Future research directions. The main limitation of the proposed algorithms is that the model of the signal emitted by the source is fully known. In this case, all the methods obtained algorithmic signal processing operations considering changes in their complex amplitudes, i.e., not only the amplitude but also the phase is processed. At the same time, it is relevant to study direction-finding methods for stochastic signals described only by correlation characteristics. This case is interesting when the task of radio detection of unknown signals is performed. Further research will determine the methods of optimising the processing of such signals and obtain practical algorithms for the direction finding of stochastic signal sources.

Contribution of authors: conceptualization – **Semen Zhyla, Eduard Tserne, Anatoliy Popov**; synthesis of the optimal signal processing algorithm – **Semen Zhyla**; simulation modelling – **Denys Kolesnikov**; antenna system implementation – **Dmytro Vlasenko**, **Volodymyr Kosharskyi**; development and implementation of radio frequency paths – **Eduard Tserne**, **Hlib Cherepnin;** conducting experiments and analysing their results – **Anatoliy Popov**, **Olha Inkarbaieva**; validation – **Anatoliy Popov, Semen Zhyla**; writing original draft – **Volodymyr Kosharskyi**, **Olha Inkarbaieva**; writing-review and editing – **Eduard Tserne**, **Dmytro Vlasenko**.

Conflict of interest

The authors declare that they have no conflict of interest in relation to this research, whether financial, personal, author ship or otherwise, that could affect the research and its results presented in this paper.

Financing

The work has been funded by the Ministry of Education and Science of Ukraine. The state registration number of the projects are 0123U101074 and 0123U101923.

Projects information

The project 0123U101074 is aimed at developing a cheap (up to 1 thousand US dollars), easy-to-manufacture, and highly accurate on-board radar system for determining the angular position of a source of interfering radio radiation. The peculiarities and novelty of this project are based on the statistical optimization of signal-processing algorithms in information and measurement systems and the methods of combining measurements from different sensors. Thus, the optimal methods determine the radio system structure, and the combination methods determine the logic of the on-board microcomputer.

In general, the project's objectives include: synthesizing signal processing algorithms for amplitude and phase direction finders, as well as possible combinations of them; developing on-board antenna systems for direction finders; developing high-frequency paths for selected types of direction finders that allow directions to be determined from radio sources over a wide range of distances; and developing systems for digitizing analog signals and their subsequent digital processing. This paper is devoted to solving some of these problems. In future work, we will consider the issue of automatic control of covered UAVs by considering the direction-finding results of radio sources.

The project 0123U101923 is aimed at developing an intelligent unmanned system for inspecting critical infrastructure facilities for optical tags and beacons. One of the parts of the complex is a direction-finding system for detecting low-power radio sources over several radio wavelengths, which can be based on the proposed direction finder.

This project covers a wide range of issues related to the application of advances in the statistical theory of

ISSN 1814-4225 (print)
ISSN 2663-2012 (online)

synthesis of radio engineering systems, detection and measurement of the coordinates of weak signal sources against the background of noise and interference in a wide range of radio frequencies, identification of informative attributes of optically contrasting markers against the background of the terrain, application of the achievements of artificial intelligence theory, in particular the method of probabilistic filtering of signals and images in combination with various types of artificial neural networks. The project's peculiarity is its practical focus on synthesizing the optimal structure of an onboard system for automatic inspection of critical infrastructure facilities, taking into account the possibility of manufacturing the system based on a modern element base available for purchase

Data availability

The manuscript has no associated data.

Use of Artificial Intelligence

The authors confirm that they did not use artificial intelligence methods while creating the presented work.

All the authors have resad and agreed to the published version of this manuscript.

References

1. Ostroumov, I., Kuzmenko, N., Sushchenko, O., Averyanova, Y., Shcherbyna, O., Solomentsev, O., Yanovsky, F., & Zaliskyi, M. Ukrainian Navigational Aids Network Configuration Estimation. *Proceedings of the 2021 IEEE 16th International Conference on the Experience of Designing and Application of CAD Systems (CADSM)*, 2021, pp. 5-9. DOI: 10.1109/CADSM52681.2021.9385226.

2. Ostroumov, I., Kuzmenko, N., & Marais, K. An Accuracy and Availability Estimation of Aircraft Positioning by Navigational Aids. *Proceedings of the 2018 IEEE 5th International Conference on Methods and Systems of Navigation and Motion Control (MSNMC)*, 2018, pp. 36-40. DOI: 10.1109/MSNMC. 2018.8576276.

3. Chen, Z., Liang, J., Lu, X., & Zheng, Z. The Safety Consideration in Civil Aircraft Communication and Navigation System Development. *Proceedings of the 2024 10th International Symposium on System Security, Safety, and Reliability (ISSSR)*, 2024, pp. 66-73. DOI: 10.1109/ISSSR61934.2024.00015.

4. Peng, L., Li, H., & Li, L. Research on the new mode of "Main-Branch-End" cargo transportation under UAV distribution. *Proceedings of the 2023 IEEE 6th Information Technology, Networking, Electronic and Automation Control Conference (ITNEC)*, 2023, pp. 317-321. DOI: 10.1109/ITNEC56291.2023. 10082354.

5. Yin, W., & Wang, Y. Research on autonomous capability assessment technology for large civilian UAVs. *Proceedings of the 2021 7th International Conference on Mechanical Engineering and Automation Science (ICMEAS)*, 2021, pp. 86-90. DOI: 10.1109/ICMEAS54189.2021.00027.

6. Yakkati, R. R., Gade, A., Koduru, B. H., Pardhasaradhi, B., & Cenkeramaddi, L. R. Classification of UAVs using Time-Frequency Analysis of Remote Control Signals and CNN. *Proceedings of the 2022 IEEE International Symposium on Smart Electronic Systems (iSES)*, 2022, pp. 1-6. DOI: 10.1109/ iSES54909.2022.00014.

7. Deng, H., Wang, H., Ji, Y., Sun, X., & Cao, X. Research on UAV Detection and Classification Based on Time-Frequency Analysis and Support Vector Machine. *Proceedings of the 2023 8th International Conference on Computer and Communication Systems (ICCCS)*, *Guangzhou*, 2023, pp. 539-543. DOI: 10.1109/ICCCS57501.2023.10151387.

8. Purwanto, K. N. J., Yahya, A., Khamis, N. H., Nor, N. M., Shaari, M. R., & Sidek, A. R. M. Accuracy Comparison of Radio Direction Finder with 6 and 4 of Log Periodic Dipole Array Antennas. *Proceedings of the 2019 6th International Conference on Information Technology, Computer and Electrical Engineering (ICITACEE)*, 2019, pp. 1-4. DOI: 10.1109/ ICITACEE.2019.8904144.

9. Zhyla, S., Popov, A., Tserne, E., Mazurenko, O., Vlasenko, D., & Inkarbaieva, O., Structure Optimisation of the Amplitude Four-antenna Direction Finder with High Accuracy and Unambiguous Measurements. *Proceedings of the 2023 13th International Conference on Dependable Systems, Services and Technologies (DESSERT)*, 2023, pp. 1-6. DOI: 10.1109/DESSERT61349.2023.10416524.

10. Skinner, S., Patel, K., Pittman, J., Lebiednik, B., Vassallo, F., & Duncan, K. J. Direction Finding System using an N-Channel Software Defined Radio Implemented with a Phase Interferometry Algorithm. *Proceedings of the 2019 SoutheastCon*, 2019, pp. 1-5. DOI: 10.1109/SoutheastCon42311.2019.9020650.

11. Lee, J.-H., Kim, J.-K., Ryu, H.-K., & Park, Y. Multiple Array Spacings for an Interferometer Direction Finder With High Direction-Finding Accuracy in a Wide Range of Frequencies. *IEEE Antennas and Wireless Propagation Letters*, 2018, vol. 17, no. 4, pp. 563-566. DOI: 10.1109/LAWP.2018.2803107.

12. Tsyporenko, V. V., Tsyporenko, V. G., & Chukhov, V. V. Eksperymental'ne doslidzhennya tochnosti bezposhukovykh metodiv spektral'noho korelyasiyno-interferometrychnoho radiopelenhuvannya [Experimental study of the accuracy of search-free methods of spectral correlation-interferometric radio direction finding]. *Tekhnichna inzheneriya – Technical engineering*, 2023, vol. 92, no. 2, pp. 199–206. DOI: 10. 26642/ten-2023-2(92)-199-206.

13. Tsyporenko, V. V. Direct digital method of the spectral correlation-interferometric radio direction-finding with double correlation processing. *Proceedings of the 2013 23rd International Crimean Conference*

"Microwave & Telecommunication Technology", 2013, pp. 304-305.

14. Polikarovskykh, O., & Hula, I. Implementing the Search Algorithm of the Correlation Interferometer Direction Finder through the GNU Radio Software Platform. *Security of Infocommunication Systems and Internet of Things*, vol. 1, no. 2, article no. 2006. DOI: 10.31861/sisiot2023.2.02006.

15. Sorochan, A. G., Dobriak, D. A., & Dobriak, O. A. Doppler direction finder J-correlation processing. *Eastern-European Journal of Enterprise Technologies*, 2013, vol. 66, no. 9, pp. 4-8. DOI: 10. 15587/1729-4061.2013.19003.

16. Sedunov, A., Sedunov, N., Salloum, H., & Sutin, A. Low-cost multichannel radio direction finding system based on software-defined radio. *Proceedings of the 2022 IEEE International Symposium on Technologies for Homeland Security (HST)*, 2022, pp. 1-6. DOI: 10.1109/HST56032.2022.10025440.

17. Drake, S. P., McKerral, J. C., & Anderson, B. D. O. Single Channel Multiple Signal Classification Using Pseudo-Doppler. *IEEE Signal Processing Letters*, 2023, no. 30, pp. 1587-1591. DOI: 10.1109/LSP.2023.3327899.

18. Won, H., Isbell, K., Vanderburgh, L., Platt, J., Lee, W., & Hong, Y.-K. Developing a Direction-Finding System and Channel Sounder Using a Pseudo-Doppler Antenna Array. *IEEE Antennas and Propagation Magazine*, 2019, vol. 61, no. 4, pp. 84-89. DOI: 10.MAP.2019.2920047.

19. Won, H., Hong, Y.-K., Isbell, K., Vanderburgh, L., Platt, J., & Choi, M. Evaluation on Pseudo-Doppler Antenna Array using Software-Defined-Radio. *Proceedings of the 2019 IEEE International Symposium on Antennas and Propagation and USNC-URSI Radio Science Meeting*, 2019, pp. 1835-1836. DOI: 10.1109/ APUSNCURSINRSM.2019.8888858.

20. Sorochan, A. G. Correlation direction finder with two OMNI-directional antennas. *Proceedings of the 2013 23rd International Crimean Conference "Microwave & Telecommunication Technology"*, 2013, pp. 298-299.

21. Kozeruk, S. O., & Korzhyk, O. V. Correlation direction finder for small aircraft. *RADAP*, 2019, vol. 79, pp. 41-47. DOI: 10.20535/RADAP.2019.79. 41-47.

22. Sorochan, A. G., & Kharchenko, V. P. J-correlation direction finder with improved characteristics of a time delay meter. *Telecommunications and Radio Engineering*, 2018, vol. 77, no. 11, pp. 4-7. DOI: 10.1615/TelecomRad Eng.v77.i11.30.

23. Jiang, X., Chen, J., He, C., Yi, G., & Shuai, Y. Direction Finding Based on Spatial Spectrum Estimation with Time-Modulated Linear Array. *Proceedings of the 2020 9th Asia-Pacific Conference on Antennas and Propagation (APCAP)*, 2020, pp. 1-2. DOI: 10.1109/APCAP50217.2020.9246062.

24. Jiang, X., Ni, G., Cao, A., Shao, C., & He, C. Single-Channel Spatial Spectrum Estimation Direction Finding by the Time-Modulated Linear Array. *IEEE Antennas and Wireless Propagation Letters*, 2020, vol. 20, no. 12, pp. 2491-2495. DOI: 10.1109/LAWP. 2021.3115826.

25. Zhan, Q., Li, S., Yan, B., Cao, A., Bai, X., & He, C. Spatial Spectrum Direction Finding by Programmable Metasurface With Time Modulation. *IEEE Antennas and Wireless Propagation Letters*, 2024 vol. 23, no. 2, pp. 458-462. DOI: 10.1109/LAWP. 2023.3311425.

26. Volosyuk, V. K., & Kravchenko, V. F. *Statisticheskaya teoriya radiotekhnicheskikh sistem distantsionnogo zondirovaniya i radiolokatsii* [Statistical Theory of Radio-Engineering Systems of Remote Sensing and Radar]. Moscow, Fizmatlit Publ., 2008. 704 p. (In Russian)

27. Pavlikov, V., Belousov, K., Zhyla, S., Tserne, E., Shmatko, O., Sobkolov, A., Vlasenko, D., Kosharskyi, V., Odokiienko, O., & Ruzhentsev, M. Radar imaging complex with SAR and ASR for aerospace vehicle. *Radioelektronni i komp'uterni sistemi – Radioelectronic and computer systems*, 2021, no. 3, pp. 63-78. DOI: 10.32620/reks.2021.3.06.

28. Tserne, E., Popov, A., Kovalchuk, D., Sereda, O., & Pidlisnyi, O. Four-antenna amplitude direction finder: statistical synthesis and experimental research of signal processing algorithm. *Radioelektronni i komp'uterni sistemi – Radioelectronic and computer systems*, 2023, vol. 108, no. 4, pp. 88-99. DOI: 10. 32620/reks.2023.4.08.

29. Dong, Y., Liu, Y., Jiang, Z., &Wang, X. Radiation Control Using Dipole-type Antenna for PCB Handset Applications. *Proceedings of the 2022 IEEE International Symposium on Antennas and Propagation and USNC-URSI Radio Science Meeting (AP-S/URSI)*, 2022, pp. 1026-1027. DOI: 10.1109/AP-S/USNC-URSI47032.2022.9886197.

30. Dong, J., & Wu, D. Design of Airborne VLF Dual Trailing Wire Antenna. *Proceedings of the 2023 6th International Conference on Electronics Technology (ICET)*, 2023, pp. 230-236. DOI: 10.1109/ICET58434. 2023.10211811.

31. Fukasawa, T., Nishimoto, K., Tanaka, T., Nishioka, Y., & Yoneda, N. Compact Multi Antennas with High Isolation Using Dipole and Monopole Modes. *Proceedings of the 2018 IEEE International Workshop on Electromagnetics: Applications and Student Innovation Competition (iWEM)*, 2018, pp. 1-1. DOI: 10.1109/iWEM.2018.8536613.

32. Zheng, M., Wang, H., & Hao, Y. Internal Hexa-Band Folded Monopole/Dipole/Loop Antenna With Four Resonances for Mobile Device. *IEEE Transactions on Antennas and Propagation*, 2012, vol. 60, no. 6, pp. 2880-2885. DOI: 10.1109/TAP.2012. 2194687.

33. Hosseini-Fahraji, A., & Manteghi, M. Design of a Wideband Coaxial Collinear Antenna. *Proceedings of the 2019 IEEE International Symposium on Antennas and Propagation and USNC-URSI Radio Science*

ISSN 1814-4225 (print)
ISSN 2663-2012 (online)

Meeting, 2019, pp. 2155-2156. DOI: 10.1109/APUSNCURSINRSM.2019.8889227.

34. Hamouz, P., Hazdra, P., Polivka, M., Capek, M., & Mazanek, M. Radiation efficiency and Q factor study of franklin antenna using the Theory of Characteristic Modes. *Proceedings of the 5th European Conference on Antennas and Propagation (EUCAP)*, 2011, pp. 1974-1977.

35. Sekhar, B.K.B.S.C., Kavitha, P., Srinivas, B., & Mahesh, C. Design of J-Pole Antenna for Receiving ADS-B Signals. *Proceedings of the 2022 International Conference on Futuristic Technologies (INCOFT)*, 2022, pp. 1-5. DOI: 10.1109/INCOFT55651.2022.10094397.

36. Analog Devices. *AD8302 Datasheet and Product Info*. Available at: https://www.analog.com/en/products/ad8302.html (accessed 25 June 2024).

37. Analog Devices. *ADL5391 Datasheet and Product Info*. Available at: https://www.analog.com/en/products/adl5391.html (accessed 25 June 2024).

38. Analog Devices. *AD8361 Datasheet and Product Info*. Available at: https://www.analog.com/en/products/ad8361.html (accessed 26 June 2024).

39. Analog Devices. *AD7608 Datasheet and Product Info*. Available at: https://www.analog.com/en/products/ad7608.html (accessed 05 July 2024).

40. Ruzhentsev, N., Zhyla, S., Pavlikov, V., Volosyuk, V., Tserne, E., Popov, A., Shmatko, O., Ostroumov, I., Kuzmenko, N., Dergachov, K., Sushchenko, O., Averyanova, Y., Zaliskyi, M., Solomentsev, O., Havrylenko, O., Kuznetsov, B., & Nikitina, T. Method for Design of Magnetic Field Active Silencing System Based on Robust Meta Model. *Proceedings of the Data Science and Security (IDSCS 2023)*, 2023, pp. 103–111. DOI: 10.1007/978-981-97-0975-5_9.

41. Ruzhentsev, N., Zhyla, S., Pavlikov, V., Volosyuk, V., Tserne, E., Popov, A., Shmatko, O., Ostroumov, I., Kuzmenko, N., Dergachov, K., Sushchenko, O., Averyanova, Y., Zaliskyi, M., Solomentsev, O., Havrylenko, O., Kuznetsov, B., & Nikitina, T. Algorithm of Robust Control for Multi-stand Rolling Mill Strip Based on Stochastic Multi-swarm Multi-agent Optimization. *Proceedings of the Data Science and Security (IDSCS 2023)*, 2023, pp. 103–111. DOI: 10.1007/978-981-97-0975-5_22.

Received 11.03.2024, Accepted 20.08.2024

БОРТОВИЙ РАДІОЛОКАЦІЙНИЙ КОМПЛЕКС ВИСОКОТОЧНОГО ПЕЛЕНГУВАННЯ ДЖЕРЕЛ РАДІОВИПРОМІНЮВАННЯ ДЛЯ АВТОНОМНОГО ПРИВЕДЕННЯ ДО НИХ КРИЛАТИХ БПЛА

Е. О. Черне, С. С. Жила, А. В. Попов, Д. С. Власенко, Д. В. Колесніков, О. С. Інкарбаєва, В. В. Кошарський, Г. С. Черепнін

Предметом статті є проєктування дешевого, простого і водночас високоточного бортового радіолокаційного комплексу визначення кутового положення станцій випромінювання радіосигналів для подальшого формування команд приведення БПЛА в задану ділянку простору. **Мета дослідження** полягає в розроблені високоточних алгоритмів функціонування, практичних рекомендацій з реалізації та проведення експериментальних вимірювань основних параметрів бортового радіопеленгатору джерел радіовипромінювання, що розміщений на крилатих БПЛА. **Завдання**, на вирішення яких спрямовано дослідження: 1) аналіз статистичної теорії оптимізації алгоритмів оброблення сигналів в радіолокаційних системах, 2) синтез алгоритмів пеленгації джерел радіовимірювань, що здатні одночасно виконувати вимірювання з високою точністю і в широкому діапазоні кутів однозначних вимірювань, 3) синтез структурної схеми радіопеленгатору і її імітаційне моделювання, 4) проєктування серії приймальних антен радіопеленгаторів, що здатні працювати відокремлено і в комплексі, 5) обґрунтування вибору комплектуючих для вхідних трактів приймачів, параметрів АЦП та мікрокомп'ютерів, що складають основні вузли радіолокаційного комплексу, 6) виготовлення робочого макету радіолокаційного комплексу, 7) проведення експериментальних вимірювань в лабораторних умовах. **Методи** вирішення поставлених завдань ґрунтуються на статистичній теорії оптимізації радіотехнічних систем дистанційного зондування та радіолокації, існуючих програмних засобах імітаційного моделювання та теорії радіовимірювань. **Основна ідея** створення дешевого, простого і водночас високоточного бортового радіолокаційного комплексу пеленгації радіовипромінювача полягає в комплексуванні результатів вимірювань кутових положень з декількох амплітудних і фазового вимірювачів. Такий підхід дозволить створити просту у використані та реалізації радіосистему з перевагами, що об'єднуються від різних вимірювачів. **Отримані наступні результати:** 1) теоретичними дослідженнями та імітаційним моделюванням підтверджено, що комплексуючи вимірювання з двоантенного амплітудного пеленгатору з вузькими діаграмами, двоантенного пеленгатору з широкими діаграмами і двоантенного фазового пеленгатору вдається досягнути одночасно високої точності й широкого діапазону однозначних вимірювань, 2) розроблено радіолокаційний комплекс на дешевій та загальнодоступній елементній базі, 3) розроблено серію антен, що можуть встановлюватися під крила БПЛА, 4) експериментальними дослідженнями підтверджено працездатність комплексної обробки сигналів в бортовому шести антенному радіопеленгаторі. Матеріал даної роботи є основою для подальших експериментальних розробок радіопеленгаторів різного призначення, відкриває можливості для подолання протиріччя між точністю та діапазоном однозначних вимірювань, висвітлює додатковий напрямок підвищення автономності руху крилатих БПЛА.

Ключові слова: багатоантенні пеленгатори, статистична оптимізація, оптимальне оброблення сигналів, експериментальні вимірювання.

Черне Едуард Олексійович – д-р філософії, доц. каф. аерокосмічних радіоелектронних систем, Національний аерокосмічний університет ім. М. Є. Жуковського "Харківський авіаційний інститут", Харків, Україна.

Жила Семен Сергійович – д-р техн. наук, зав. каф. аерокосмічних радіоелектронних систем, Національний аерокосмічний університет ім. М. Є. Жуковського "Харківський авіаційний інститут", Харків, Україна.

Попов Анатолій Владиславович – д-р техн. наук, доц., проф. каф. аерокосмічних радіоелектронних систем, Національний аерокосмічний університет ім. М. Є. Жуковського "Харківський авіаційний інститут", Харків, Україна.

Власенко Дмитро Сергійович – д-р філософії, доц. каф. аерокосмічних радіоелектронних систем, Національний аерокосмічний університет ім. М. Є. Жуковського "Харківський авіаційний інститут", Харків, Україна.

Колесніков Денис Вікторович – д-р філософії, доц. каф. аерокосмічних радіоелектронних систем, Національний аерокосмічний університет ім. М. Є. Жуковського "Харківський авіаційний інститут", Харків, Україна.

Інкарбаєва Ольга Сергіївна – д-р філософії, доц. каф. аерокосмічних радіоелектронних систем, Національний аерокосмічний університет ім. М. Є. Жуковського "Харківський авіаційний інститут", Харків, Україна.

Кошарський Володимир Віталійович – д-р філософії, доц. каф. аерокосмічних радіоелектронних систем, Національний аерокосмічний університет ім. М. Є. Жуковського "Харківський авіаційний інститут", Харків, Україна.

Черепнін Гліб Сергійович – д-р філософії, доц. каф. аерокосмічних радіоелектронних систем, Національний аерокосмічний університет ім. М. Є. Жуковського "Харківський авіаційний інститут", Харків, Україна.

Eduard Tserne – PhD in Telecommunications and radio engineering, Associate Professor at the Aerospace Radio-Electronic Systems Department, National Aerospace University "Kharkiv Aviation Institute", Kharkiv, Ukraine,
e-mail: e.tserne@khai.edu, ORCID: 0000-0003-0709-2238.

Semen Zhyla – D.Sc. in Radioengineering, Head of the Aerospace Radio-electronic Systems Department, National Aerospace University "Kharkiv Aviation Institute", Kharkiv, Ukraine,
e-mail: s.zhyla@khai.edu, ORCID: 0000-0003-2989-8988.

Anatoliy Popov – D.Sc. in Radioengineerng, Associate Professor at the Aerospace Radio-Electronic Systems Department, National Aerospace University "Kharkiv Aviation Institute", Kharkiv, Ukraine,
e-mail: a.v.popov@khai.edu, ORCID: 0000-0003-0715-3870.

Dmytro Vlasenko – PhD in Telecommunications and Radioengineering, Associate Professor at the Aerospace Radio-Electronic Systems Department, National Aerospace University "Kharkiv Aviation Institute", Kharkiv, Ukraine,
e-mail: d.vlasenko@khai.edu, ORCID: 0000-0002-6118-2173.

Denys Kolesnikov – PhD in Telecommunications and Radioengineering, Associate Professor at the Aerospace Radio-Electronic Systems Department, National Aerospace University "Kharkiv Aviation Institute", Kharkiv, Ukraine,
e-mail d.kolesnikov@khai.edu, ORCID: 0000-0002-0135-2695.

Olha Inkarbaieva – PhD in Telecommunications and Radioengineering, Associate Professor at the Aerospace Radio-Electronic Systems Department, National Aerospace University "Kharkiv Aviation Institute", Kharkiv, Ukraine,
e-mail: o.inkarbayeva@khai.edu, ORCID: 0000-0002-2547-8241.

Volodymyr Kosharskyi – PhD in Telecommunications and Radioengineering, Associate Professor at the Aerospace Radio-Electronic Systems Department, National Aerospace University "Kharkiv Aviation Institute", Kharkiv, Ukraine,
e-mail: v.kosharsky@khai.edu, ORCID: 0000-0002-8569-2047.

Hlib Cherepnin – PhD in Telecommunications and Radioengineering, Associate Professor at the Aerospace Radio-Electronic Systems Department, National Aerospace University "Kharkiv Aviation Institute", Kharkiv, Ukraine,
e-mail: g.cherepnin@khai.edu, ORCID: 0000-0003-1245-0933.